Design guide for RF low-noise transistors in global navigation satellite systems

RF bipolar transistors

About this document

Scope and purpose

This application note provides application circuit design examples with Infineon's low-noise silicon germanium: carbon (SiGe:C) transistors for global navigation satellite system (GNSS) low noise amplifiers (LNA). In this document the transistor-based LNA schematics, PCB layouts and measurement results are presented. This document is relevant to the following low-noise transistors:

- BFP640ESD — Navigation systems and satellite radio
- BFP740 — Low-noise transistor for WLAN
- BFP740ESD — Low-noise transistor for WLAN
- BFP842ESD — Low-noise transistor for WLAN
- BFP640FESD — Navigation systems and satellite radio
- BFP740F — Low-noise transistor for WLAN
- BFP740FESD — Low-noise transistor for WLAN
- BGB707L7ESD — Low-noise transistor for WLAN
- BGB741L7ESD — Navigation systems and satellite radio

Intended audience

This document is intended for engineers who need to design LNAs for GNSS applications.

Table of contents

1 Introduction

1.1 GNSS receiver front end

Today, GNSS is much more than the global positioning system (GPS). More and more satellite systems are providing the navigation service, such as GLONASS, BeiDou and Galileo. The service from GNSS systems has become an important part of our daily life, for example in the context of digital maps on smartphones and positioning in automotive navigators.

The GNSS service quality depends on received signal level and the level of background noise. The GNSS satellites are at an orbit altitude of more than 20,000 km from the Earth's surface. After taking losses (atmospheric, antenna, etc.) into account, the received GNSS signal strength on the ground is very low around −130 dBm. In some challenging environments, such as urban streets, roads in woods and indoors, the received signal level is further attenuated due to the obstructed reception paths. The ability of the GNSS device to receive such low signal strength and provide meaningful information to the end-user depends strongly on the first stage signal amplification with a low measure of noise figure (NF) in the receiver chain. However, in some applications, the GNSS receiver has to be placed far away from the antenna. The additional connection loss between the antenna and receiver causes the performance to deteriorate dramatically.

An LNA close to the receiver antenna provides the solution and improves the receiver's sensitivity to the weak signals from satellites. Therefore, the GNSS receiver benefits from a shorter time-to-first-fix (TTFF), which is the time spent waiting for acquiring satellite signals and calculating the current position. The combination of antenna and LNA, together with filters, builds up the GNSS receiver radio frequency (RF) front end, sometimes referred to as the "active antenna".

Depending on the system specification emphasis of NF, gain or out-of-band interference, the sequence of LNA and filters in the GNSS RF front end can be different. The following figure shows two of the most common configurations.

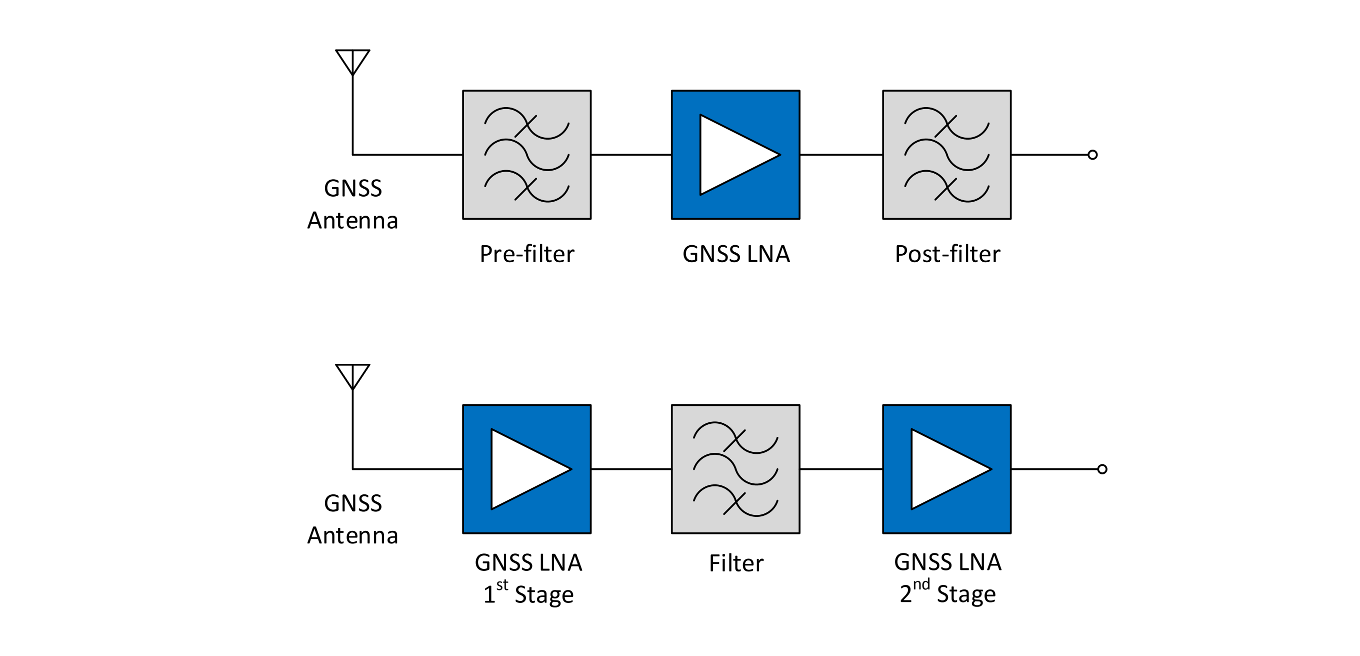

Figure 1 Block diagram examples of GNSS RF front end

1.2 Infineon RF transistor family

Infineon Technologies provides high-performance RF transistors targeting GNSS LNA applications. Infineon's reliable high-volume RF transistors offer exceptionally low NF, high gain and high linearity at low power consumption levels for RF applications. The sixth- and seventh-generation and the high-performance eighth-generation transistors are based on robust ultra low-noise SiGe:C technologies. Their optimized inner transistor cell structure leads to best-in-class power gains and NFs at high frequencies, including GNSS bands. The transistors optimize the design flexibility for customer requirements.

The BGB707L7ESD and BGB741L7ESD are SiGe:C low-noise monolithic microwave integrated circuits (MMICs) with integrated ESD protection and active biasing. The devices are as flexible as discrete transistors and feature high gain, reduced power consumption and very low distortion for a very wide range of applications.

2 GNSS LNA circuits with SOT343 packaged transistors

2.1 Performance overview

The following table reports the GNSS LNAs' performance with RF low-noise bipolar transistors in a SOT343 package measured at 1575 MHz.

Table 1 Summary of measurement results for the GNSS LNAs with SOT343 packaged transistors

Parameter	Symbol	Value				Unit	Notes
Device		BFP640ESD	BFP740	BFP740ESD	BFP842ESD		
Bias voltage	V_{CC}	3.0	3.0	3.0	3.0	V	
Bias current	I_{CC}	8.0	9.8	9.4	10.9	mA	
Gain	G	17.8	19.1	18.5	17.9	dB	
NF	NF	0.82	0.71	0.72	0.66	dB	
Input return loss	RL_{in}	16.2	14.4	9.7	10.9	dB	
Output return loss	RL_{out}	10.3	11.2	9.9	10.7	dB	
Reverse isolation	ISO_{rev}	29.2	29.8	30.5	28.7	dB	
Input 1 dB compression point	IP_{1dB}	-17.1	-16.4	-18.1	-13.0	dBm	
Output 1 dB compression point	OP_{1dB}	-0.3	1.7	-0.6	3.8	dBm	
Input third-order intercept point	IIP_3	2.7	2.6	0.8	2.7	dBm	
Output third-order intercept point	OIP_3	20.5	21.7	19.4	20.6	dBm	P_{IN} = -30 dBm per tone f_1 = 1575 MHz f_2 = 1576 MHz
Stability	K	>1	>1	>1	>1		Measured from 10 MHz to 13 GHz

2.2 Schematic

The following figure shows the general schematic of the GNSS LNAs with SOT343 packaged RF low-noise transistors. In the schematic, the resistor R1 serves as the DC negative feedback to stabilize the biasing point, while R2 stands for transistor base bias. The circuit input matching is achieved by the network of the capacitors C1, C2 and the inductor L1. The network of L2, C4, and C5 matches the transistor to the output port. In general, R3 and R4 stabilize the circuit, whose firmness is measured up to 13 GHz.

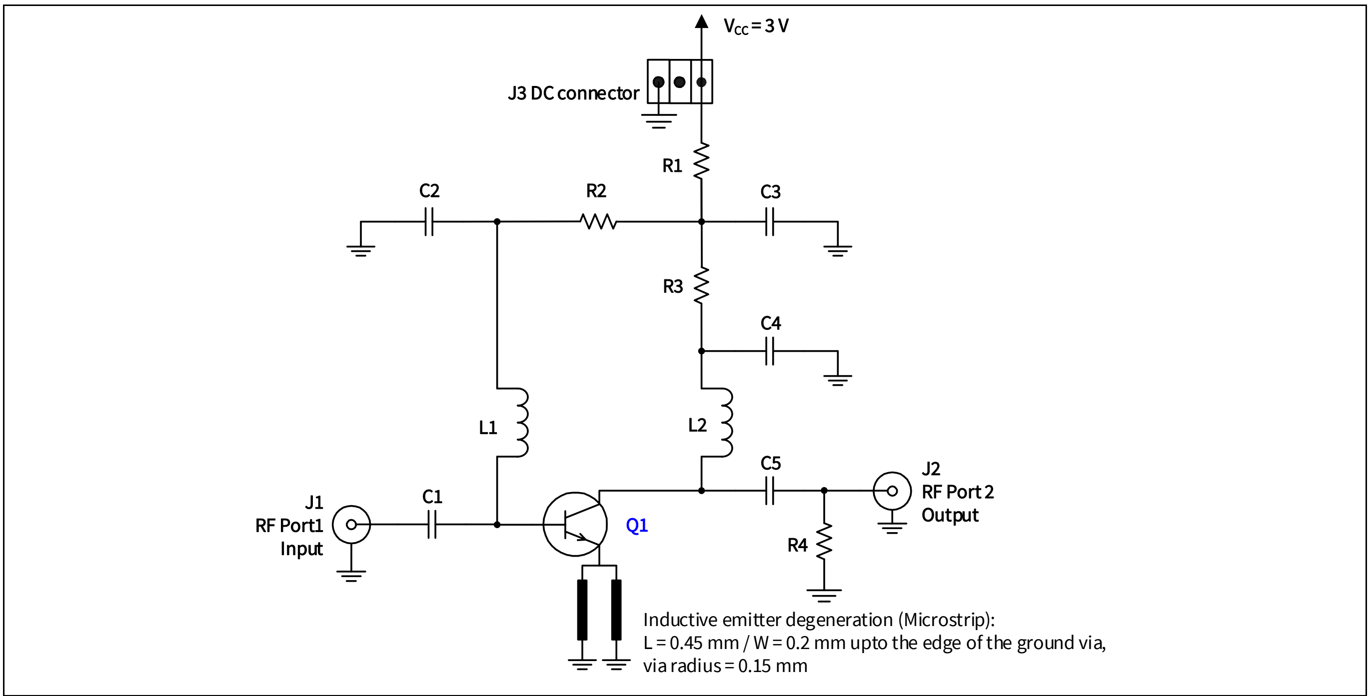

Figure 2 The GNSS LNAs' schematic with SOT343 packaged transistors

2.3 Bill of materials (BOM)

Table 2 BOM of the GNSS LNAs with SOT343 packaged transistors

Symbol	Value				Unit	Package	Manu-facturer	Comment
Q1	BFP640ESD	BFP740	BFP740ESD	BFP842ESD		SOT343	Infineon	SiGe:C transistor
C1	22	22	22	22	pF	0402	Various	Input matching and DC blocking
C2	47	47	47	47	nF	0402	Various	RF decoupling
C3	47	47	47	47	nF	0402	Various	RF decoupling
C4	5.6	5.6	n.c.[1)]	5.6	pF	0402	Various	Output matching
C5	1.8	1.8	2.7	1.5	pF	0402	Various	Output matching and DC blocking
R1	30	30	30	30	Ω	0402	Various	DC bias
R2	47	47	56	56	kΩ	0402	Various	DC bias
R3	20	20	20	20	Ω	0402	Various	Low-frequency stability improvement
R4	150	120	120	160	Ω	0402	Various	Output matching and stability improvement
L1	10	10	10	10	nH	0402	Murata LQG	Input matching
L2	8.2	8.2	8.2	8.2	nH	0402	Murata LQG	Output matching

Note: 1) Not connected (n.c.).

2.4 Evaluation board and layout information

The evaluation board for the GNSS LNAs with SOT343 packaged transistors:

- PCB material: FR4
- PCB marking: M111117

The photo of the evaluation board and the detailed description of emitter degeneration are shown in the following figure.

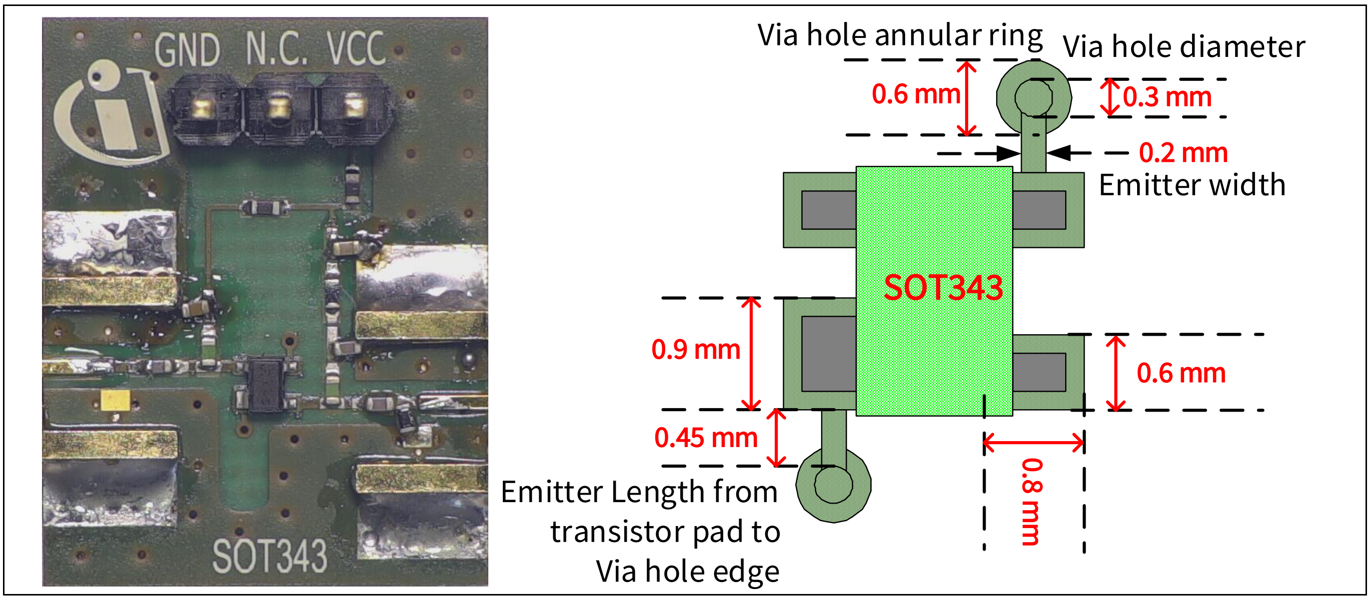

Figure 3 Photo of the SOT343 packaged transistor LNA evaluation board (left) and emitter degeneration details (right)

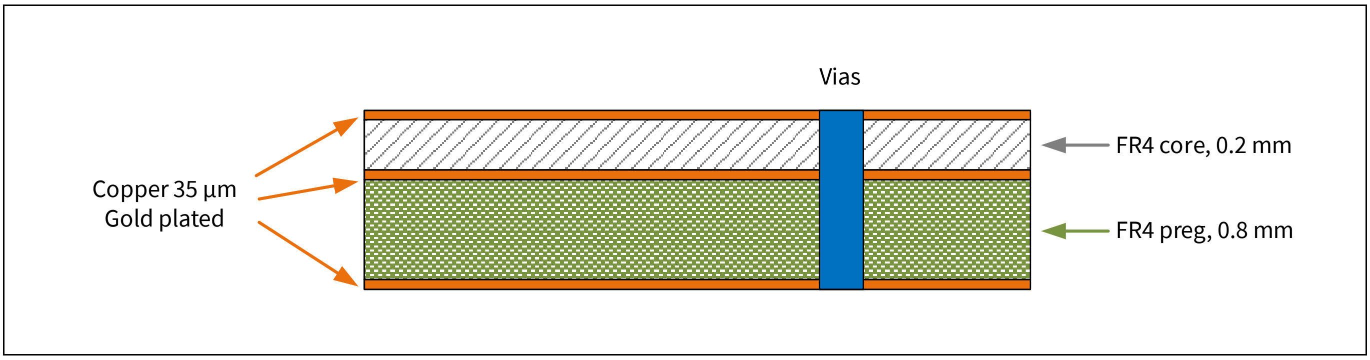

Figure 4 PCB stack information for the evaluation board M111117

2.5 Measurement results of the GNSS LNAs with SOT343 packaged transistors

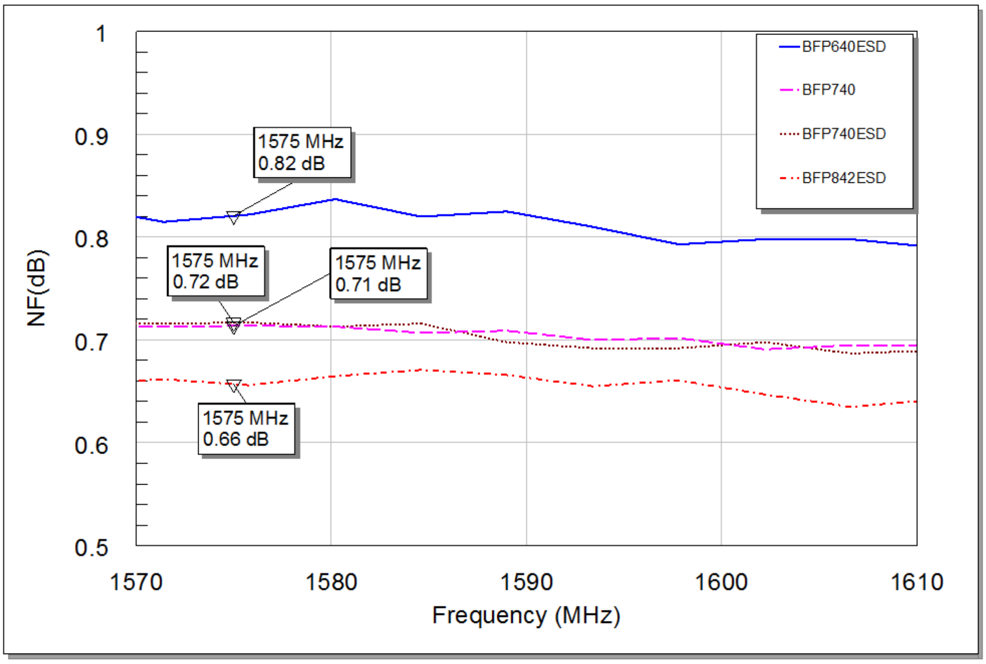

Figure 5 NF measurement of the GNSS LNAs with SOT343 packaged transistors

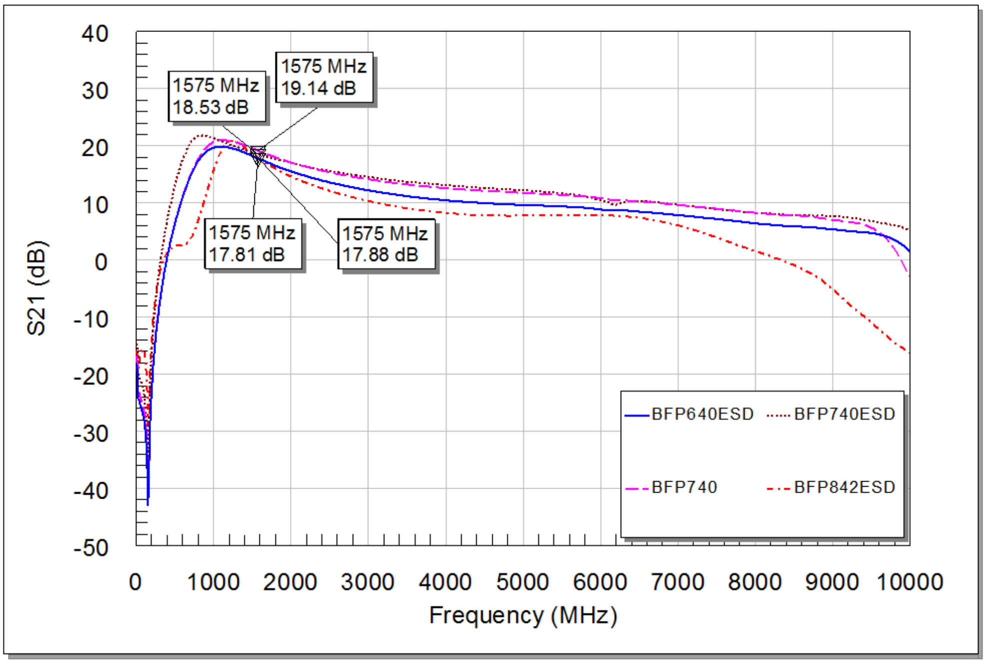

Figure 6 Small signal gain of the GNSS LNAs with SOT343 packaged transistors

Note: The graphs are generated with the AWR electronic design automation (EDA) software Microwave Office®.

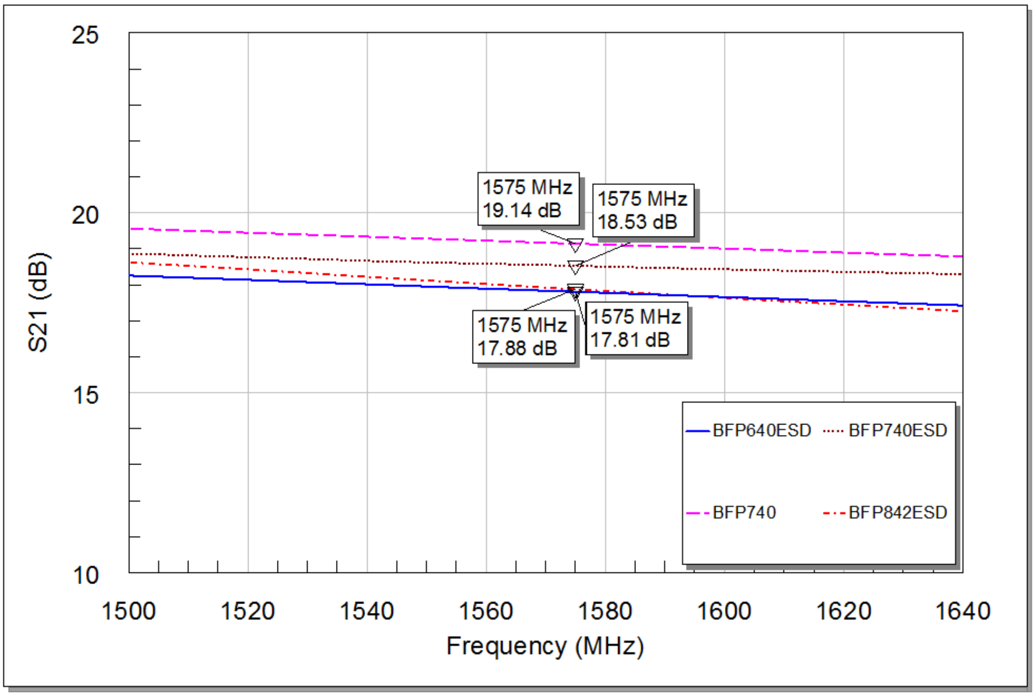

Figure 7 Small signal gain of the GNSS LNAs with SOT343 packaged transistors (detail view)

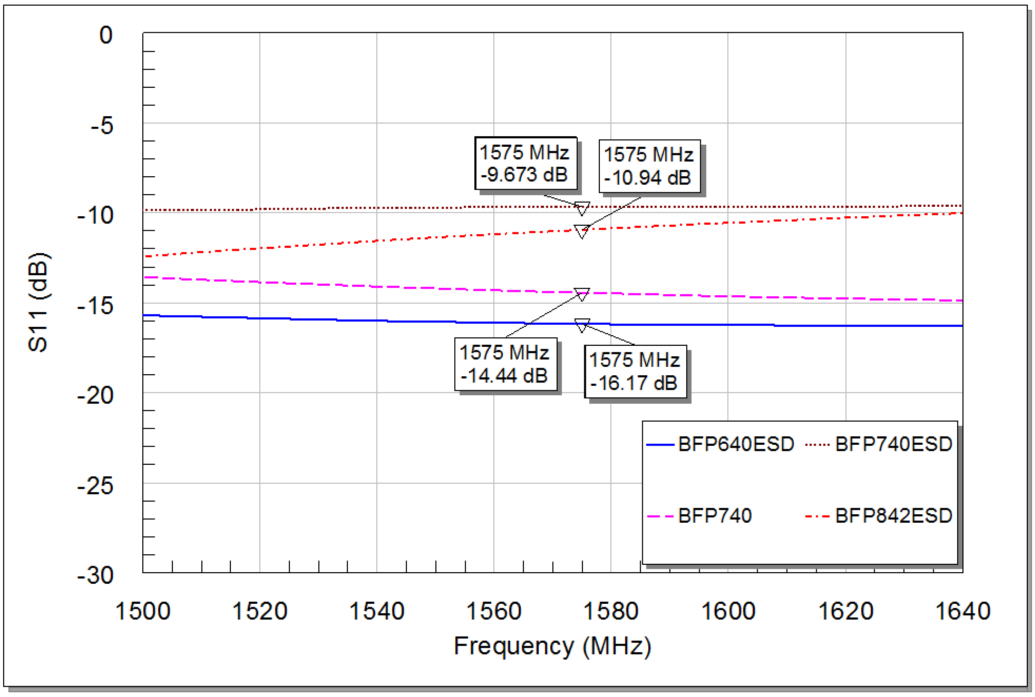

Figure 8 S_{11} of the GNSS LNAs with SOT343 packaged transistors

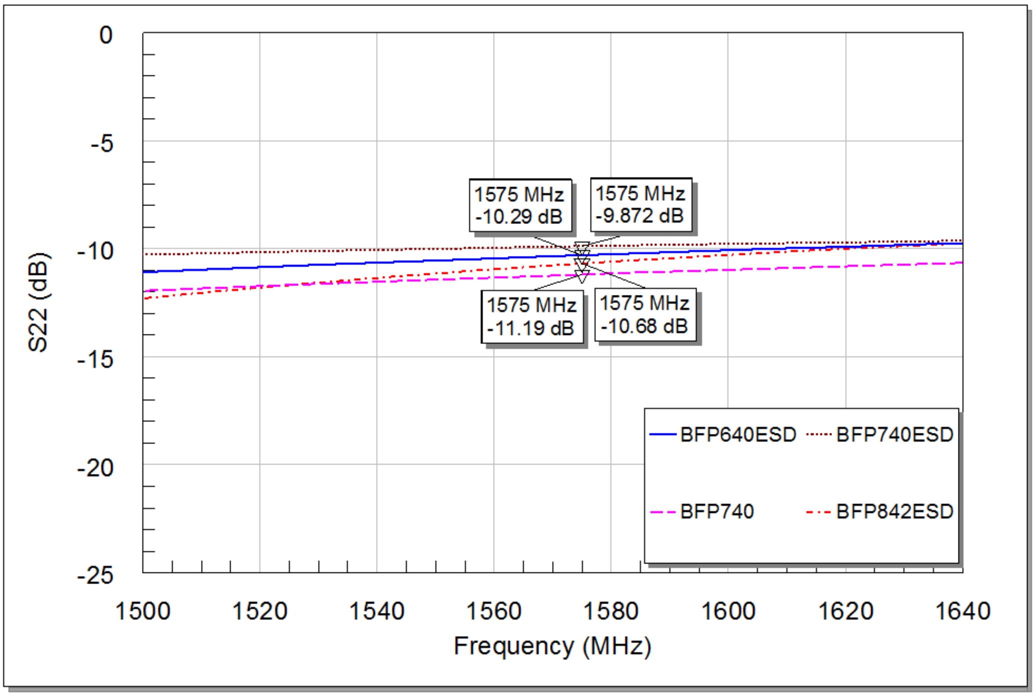

Figure 9 S_{22} of the GNSS LNAs with SOT343 packaged transistors

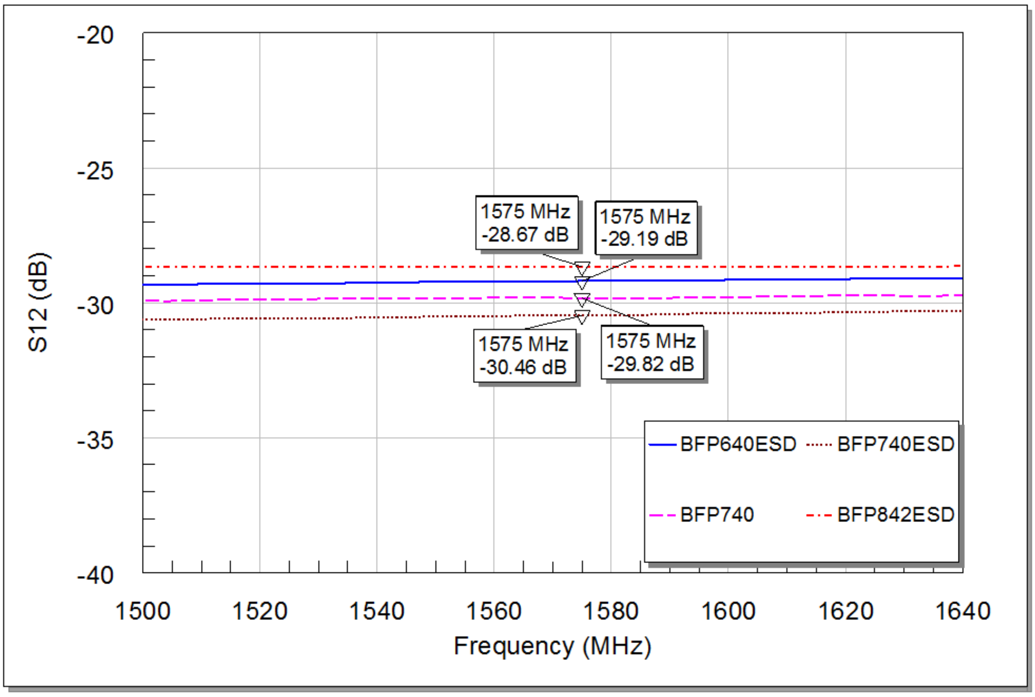

Figure 10 Reverse isolation of the GNSS LNAs with SOT343 packaged transistors

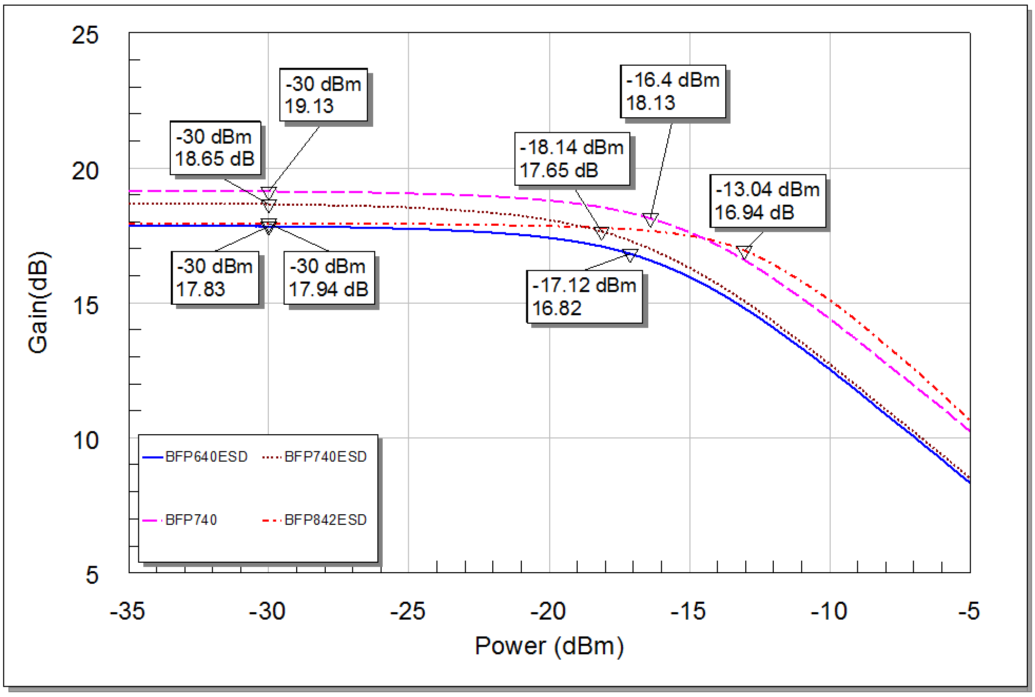

Figure 11 Input 1 dB compression point of the GNSS LNAs with SOT343 packaged transistors

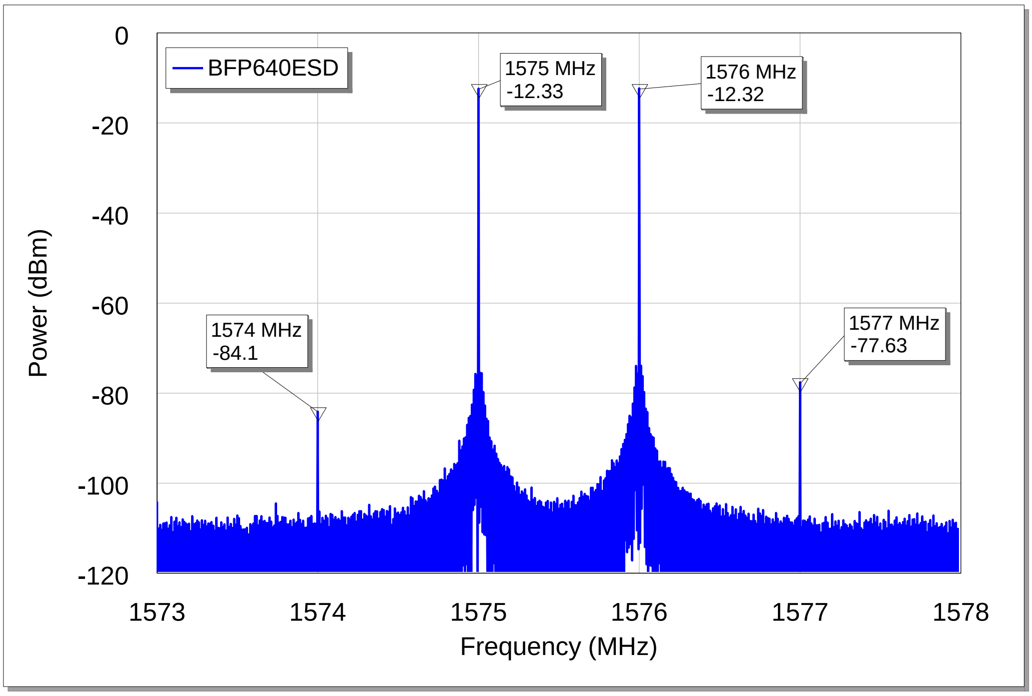

Figure 12 Output third-order intermodulation products of the GNSS LNA with transistor BFP640ESD

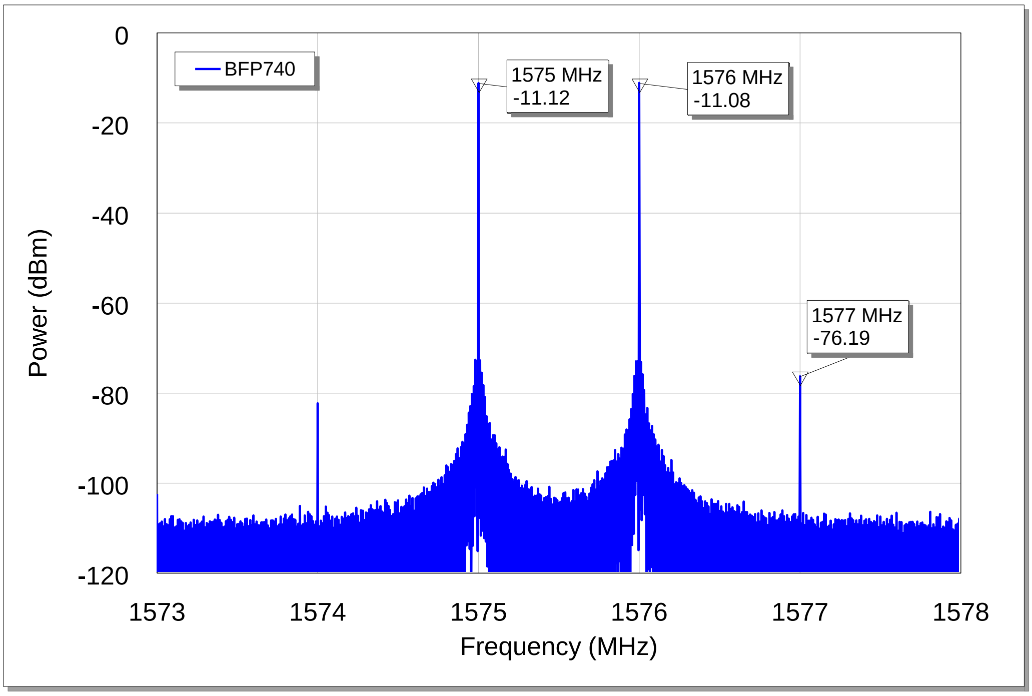

Figure 13 Output third-order intermodulation products of the GNSS LNA with transistor BFP740

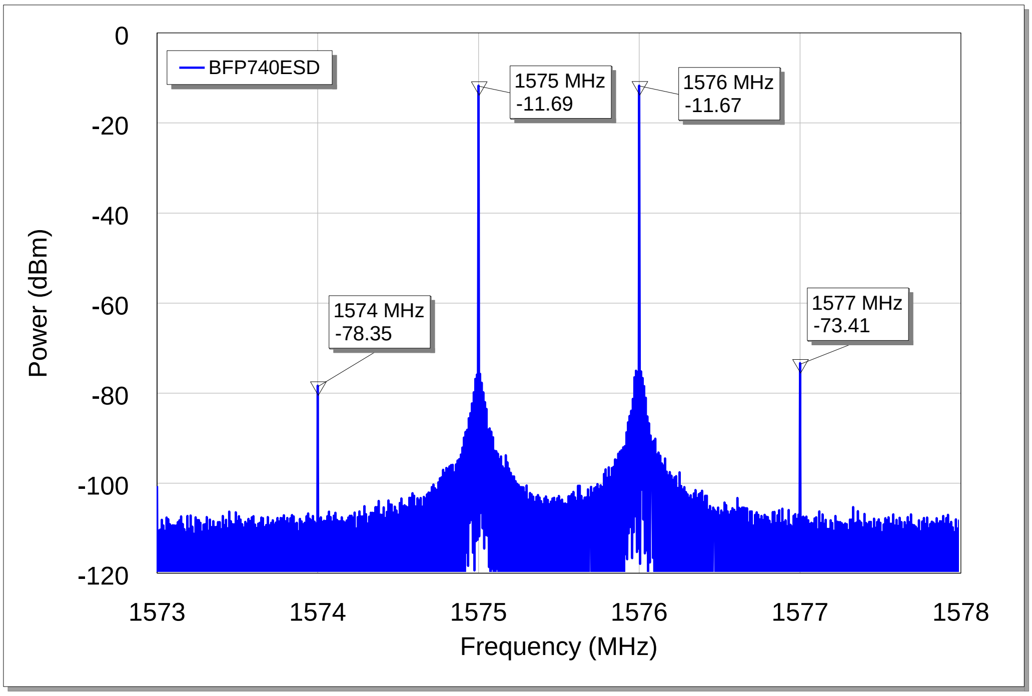

Figure 14 Output third-order intermodulation products of the GNSS LNA with transistor BFP740ESD

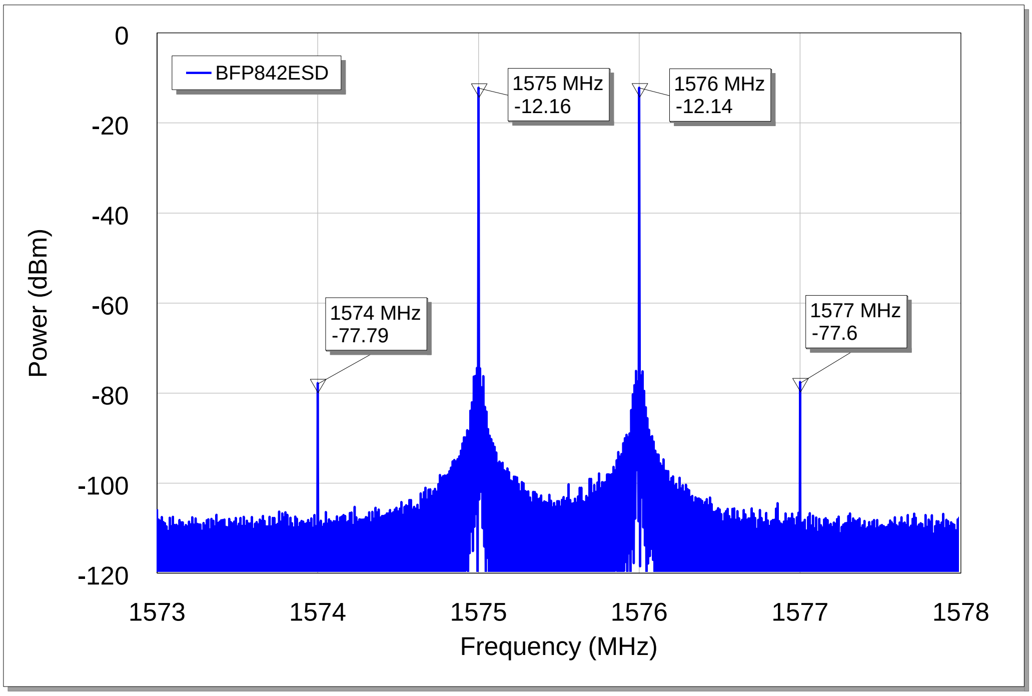

Figure 15 Output third-order intermodulation products of the GNSS LNA with transistor BFP842ESD

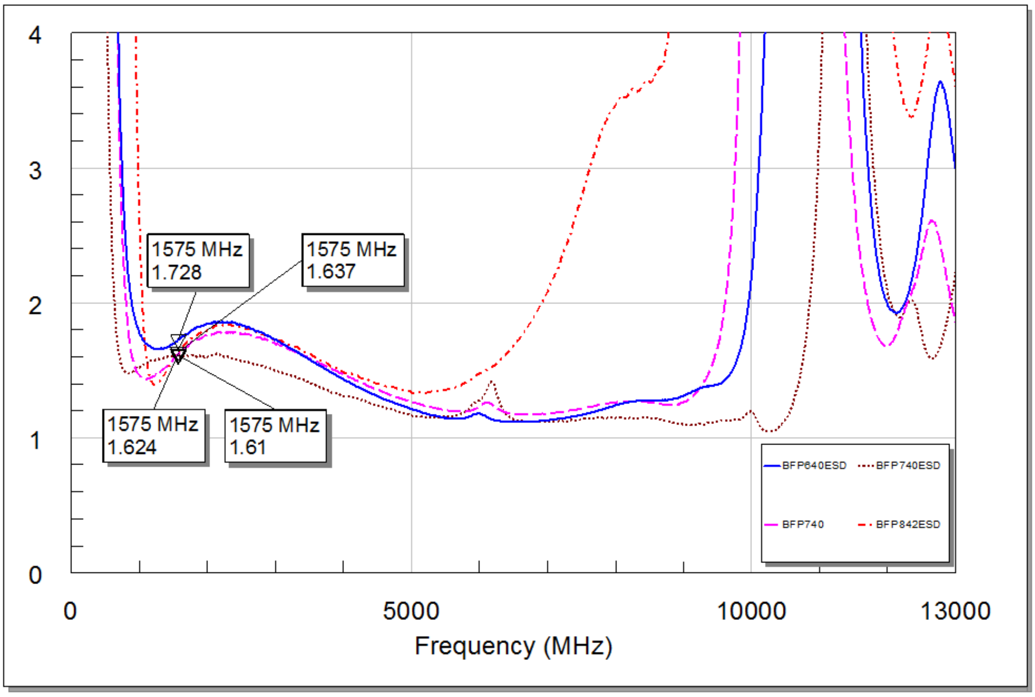

Figure 16 K-factor measurement of the GNSS LNAs with SOT343 packaged transistors

3 The GNSS LNAs with low-noise transistors in small and flat leaded TSFP packages

3.1 Performance overview

The following table shows the performance of the LNAs with RF low noise bipolar transistors in small and flat leaded TSFP packages measured at 1575 MHz.

Table 3 Summary of measurement results for the GNSS LNAs with TSFP packaged transistors

Parameter	Symbol	Value			Unit	Notes
Device		BFP640FESD	BFP740F	BFP740FESD		
Bias voltage	V_{CC}	3.0	3.0	3.0	V	
Bias current	I_{CC}	8.0	9.4	9.8	mA	
Gain	G	18.3	19.3	19.8	dB	
Noise figure	NF	0.81	0.71	0.68	dB	
Input return loss	RL_{in}	13.9	10.2	11.2	dB	
Output return loss	RL_{out}	11.6	11.8	11.4	dB	
Reverse isolation	ISO_{rev}	29.7	29.8	20.2	dB	
Input 1 dB compression point	IP_{1dB}	-17.9	-17.6	-17.3	dBm	
Output 1 dB compression point	OP_{1dB}	-0.6	0.7	1.5	dBm	
Input third-order intercept point	IIP_3	1.1	1.2	1.8	dBm	
Output third-order intercept point	OIP_3	19.4	20.5	21.6	dBm	P_{IN} = -30 dBm per tone f_1 = 1575 MHz f_2 = 1576 MHz
Stability	K	>1	>1	>1		From 10 MHz to 13 GHz

3.2 Schematic

The following figure presents the schematic of the GNSS LNAs with RF low-noise transistors in small and flat leaded TSFP packages. In the schematic, the resistor R1 serves as the DC negative feedback to stabilize the biasing points, while R2 stands for transistor base bias. The circuit input matching is achieved by the network of capacitors C1, C2 and the inductor L1. The network of L2, C5 and C4 matches the transistor to the output port. In general, R3 and R4 stabilize the circuit whose firmness is measured up to 13 GHz.

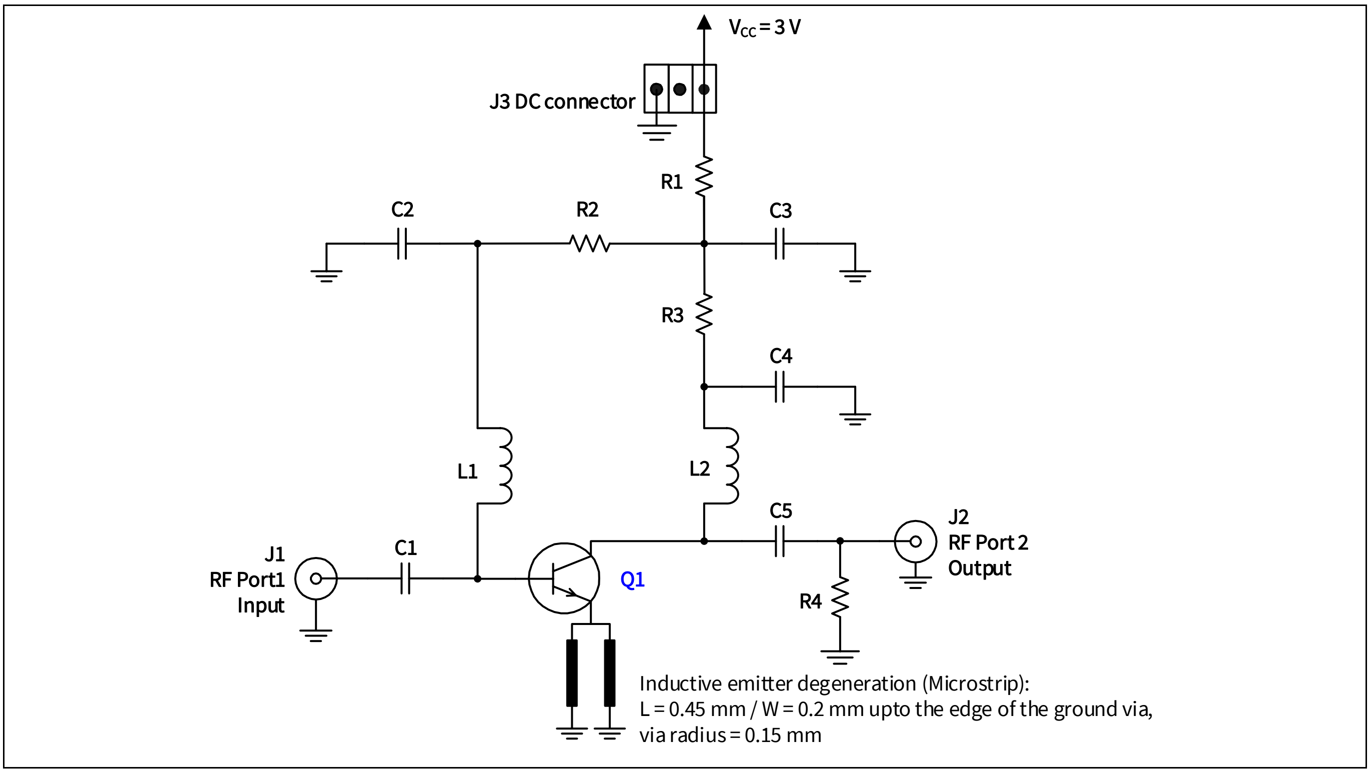

Figure 17 The GNSS LNAs' schematic with transistors in small and flat leaded TSFP packages

3.3 BOM

Table 4 BOM of the GNSS LNAs with transistors in small and flat leaded TSFP packages

Symbol	Value			Unit	Package	Manu-facturer	Comment
Q1	BFP640FESD	BFP740F	BFP740FESD		TSFP	Infineon	SiGe bipolar transistor
C1	22	22	22	pF	0402	Various	Input matching and DC blocking
C2	47	47	47	nF	0402	Various	RF decoupling
C3	47	47	47	nF	0402	Various	RF decoupling
C4	5.6	3.3	4.7	pF	0402	Various	Output matching and stability improvement
C5	1.8	1.8	1.8	pF	0402	Various	Output matching and DC blocking
R1	30	30	30	Ω	0402	Various	DC bias
R2	47	51	56	kΩ	0402	Various	DC bias
R3	30	30	30	Ω	0402	Various	Low-frequency stability improvement
R4	120	120	120	Ω	0402	Various	Output matching and high-frequency stability improvement
L1	10	10	10	nH	0402	Murata LQG	RF choke and input matching

Symbol	Value			Unit	Package	Manu-facturer	Comment
L2	8.2	8.2	8.2	nH	0402	Murata LQG	RF choke and output matching

3.4 Evaluation board and layout information

The evaluation board for the GNSS LNAs with transistors in small and flat leaded TSFP packages:

- PCB material: FR4
- PCB marking: M111118

The photo of the evaluation board and the detailed description of emitter degeneration are shown in the following figures.

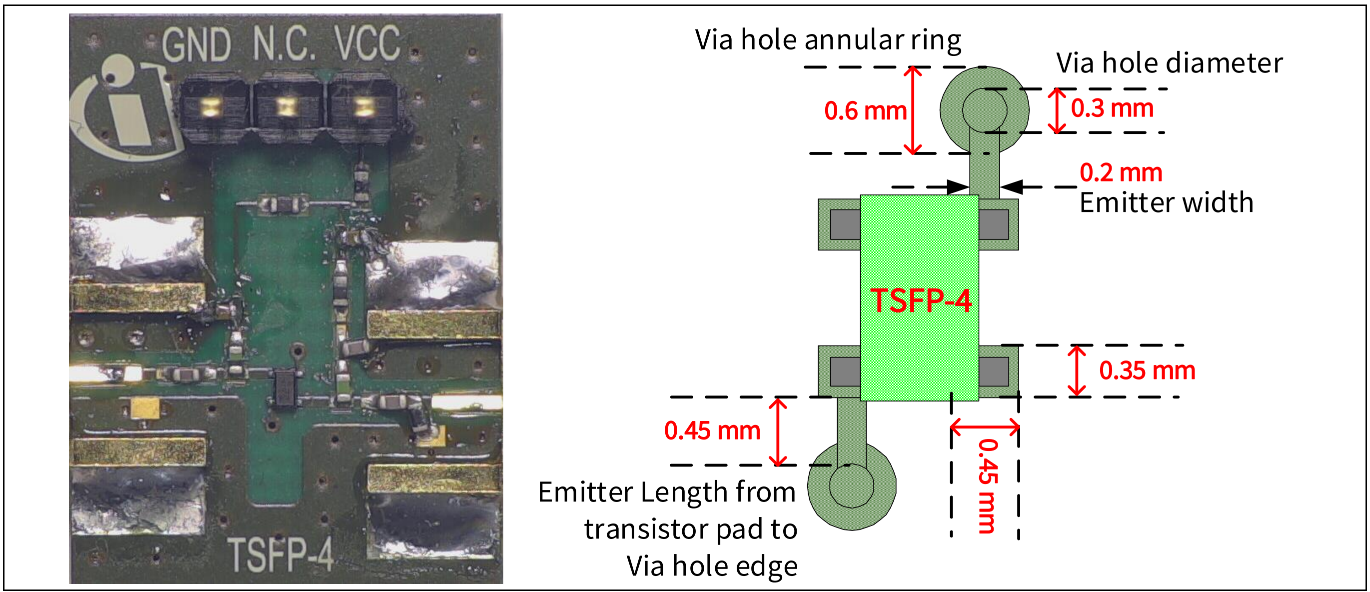

Figure 18 Photo of a small and flat leaded TSFP packaged transistor LNA evaluation board (left) and emitter degeneration details (right)

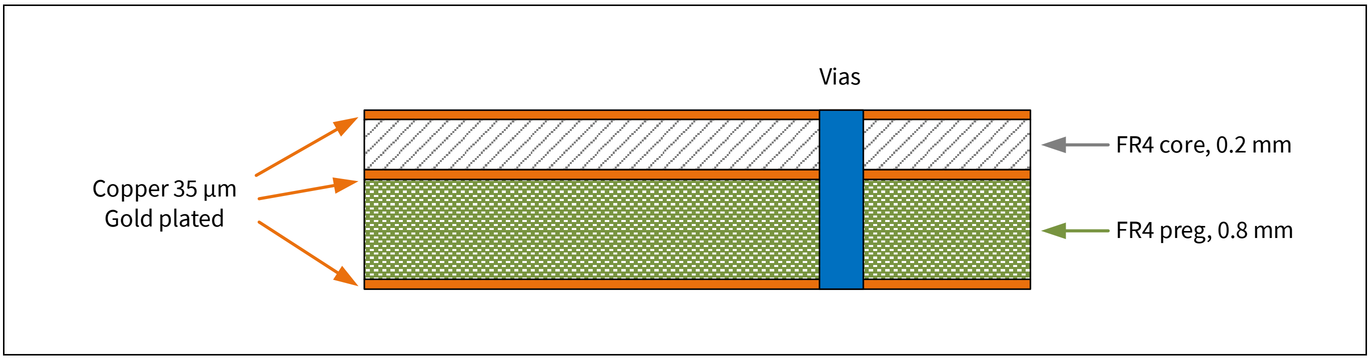

Figure 19 PCB stack information for the evaluation board M111118

3.5 Measurement results of the GNSS LNAs with low-noise transistors in small and flat leaded TSFP packages

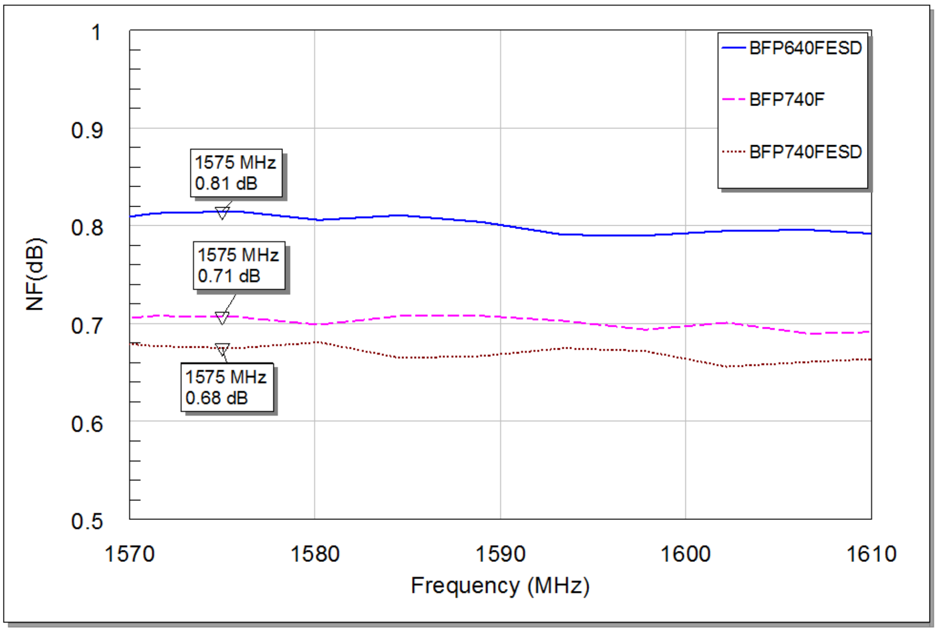

Figure 20 NF measurement of the GNSS LNAs with transistors in small and flat leaded TSFP packages

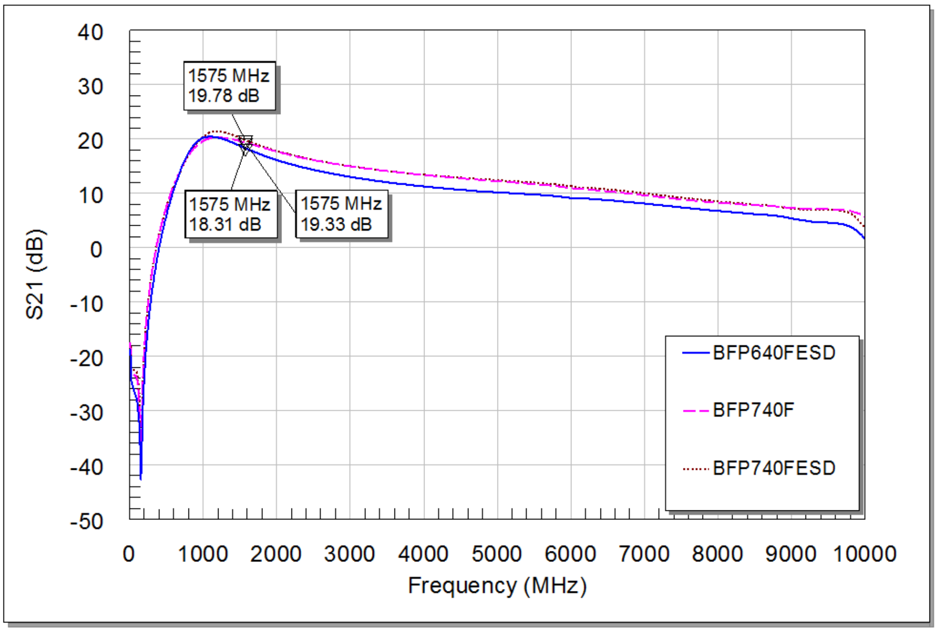

Figure 21 Small signal gain measurement of the GNSS LNAs with transistors in small and flat leaded TSFP packages

Note: The graphs are generated with the AWR EDA software Microwave Office®.

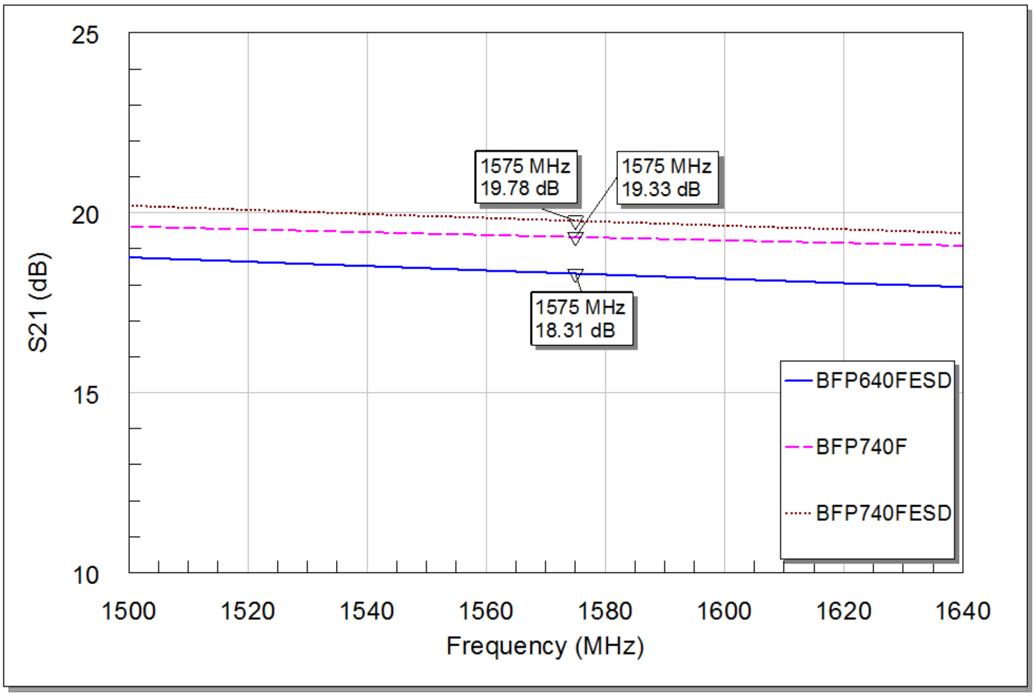

Figure 22 Small signal gain measurement of GNSS LNAs with transistors in small and flat leaded TSFP packages (detail view)

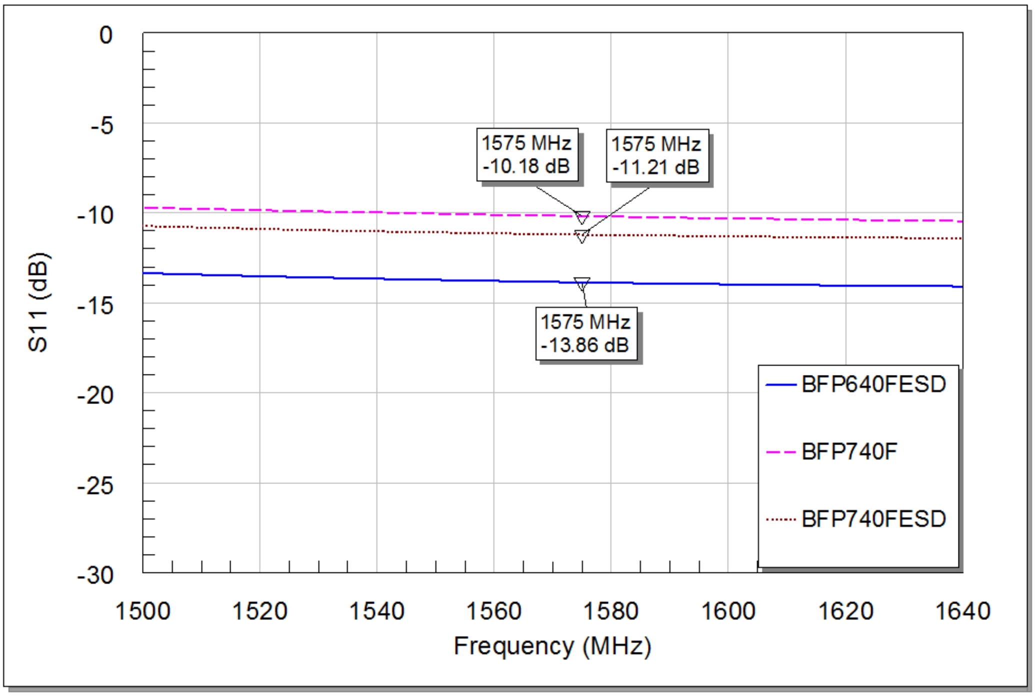

Figure 23 S_{11} measurement of the GNSS LNAs with transistors in small and flat leaded TSFP packages

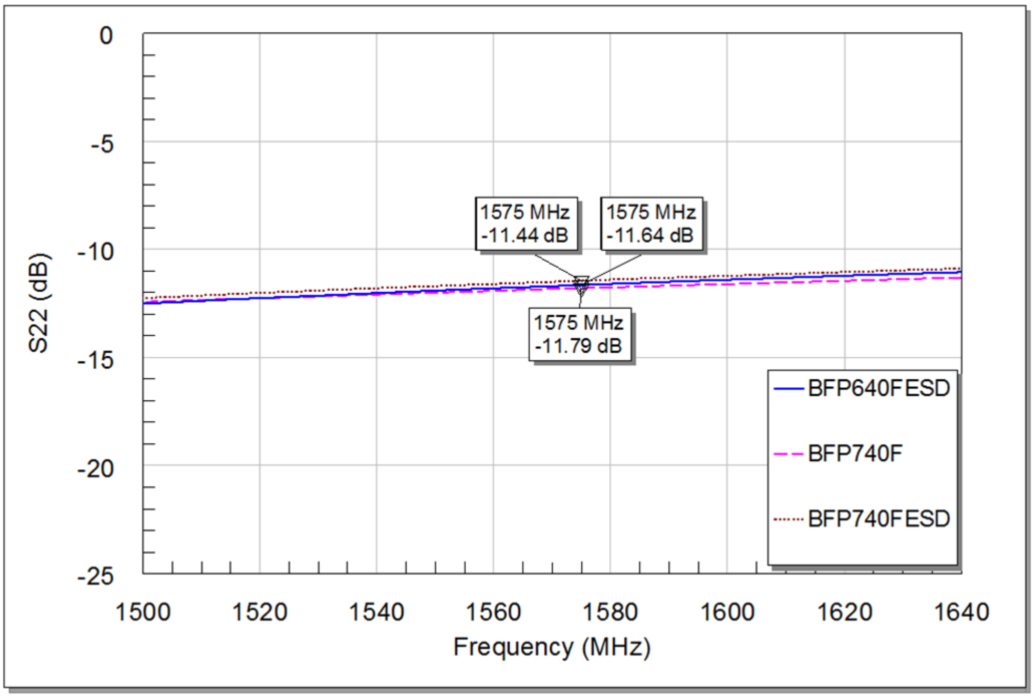

Figure 24 S_{22} measurement of the GNSS LNAs with transistors in small and flat leaded TSFP packages

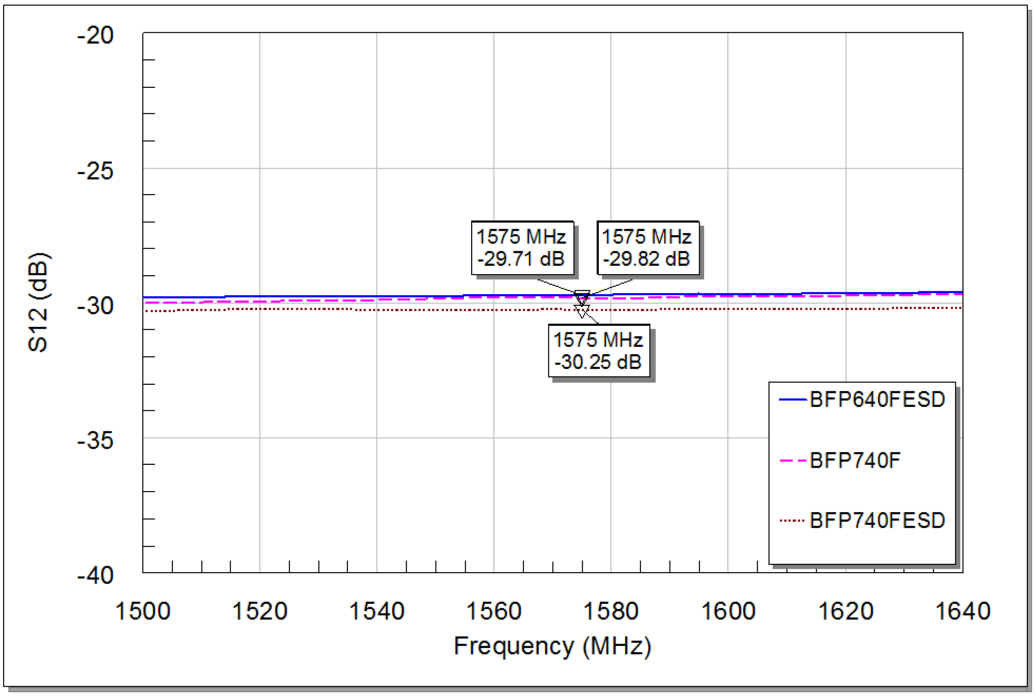

Figure 25 Reverse isolation measurement of the GNSS LNAs with transistors in small and flat leaded TSFP packages

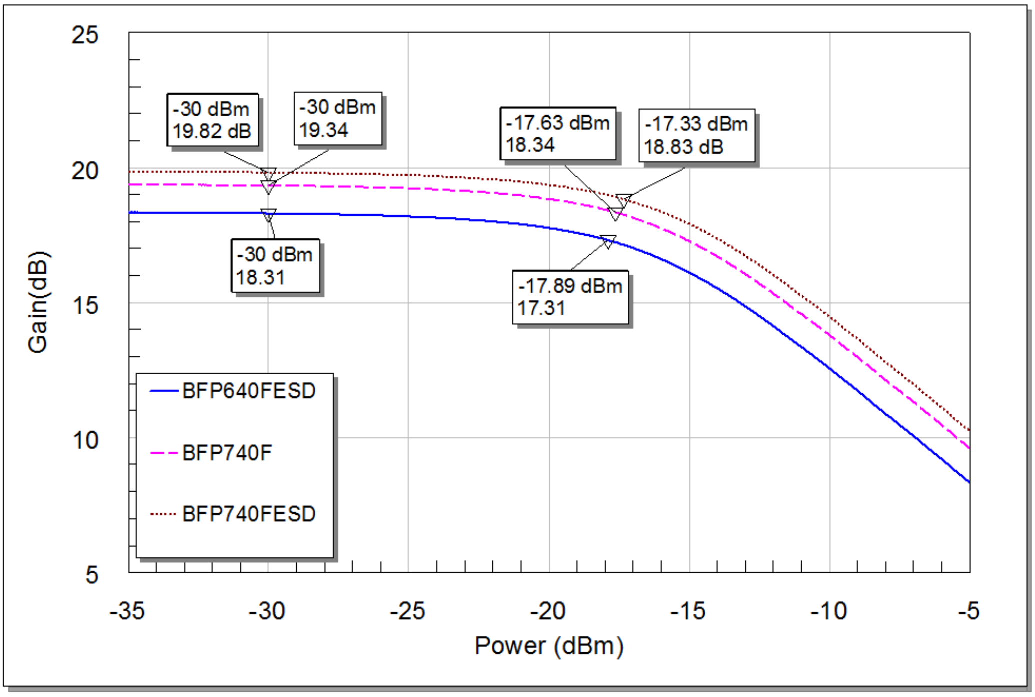

Figure 26 Input 1 dB gain compression point measurement of the GNSS LNAs with transistors in small and flat leaded TSFP packages

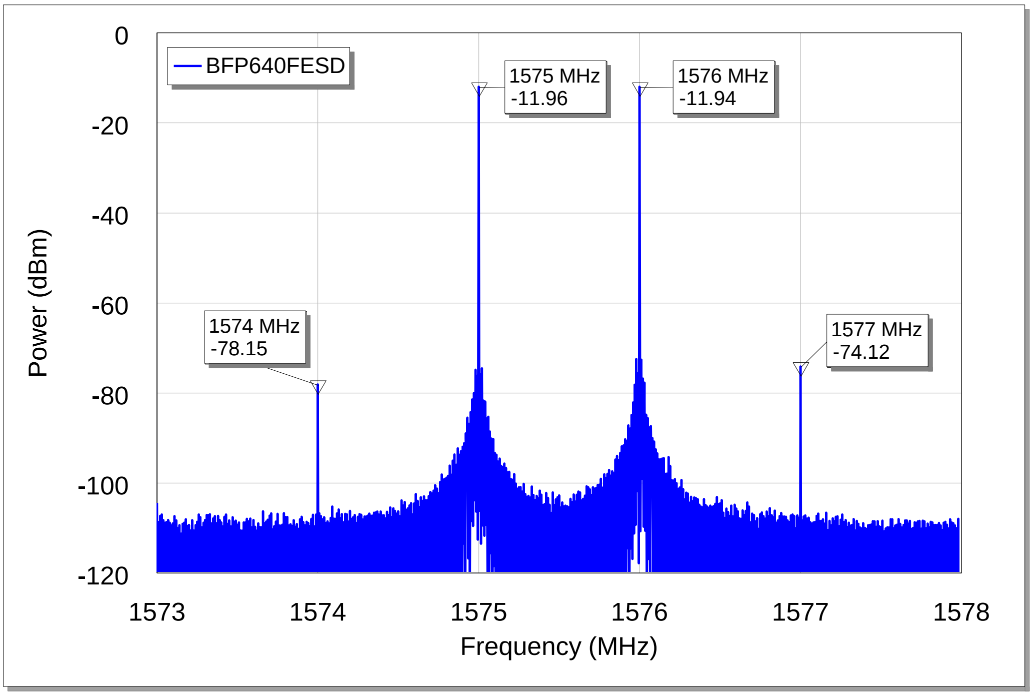

Figure 27 Output third-order intermodulation distortion product of the GNSS LNA with BFP640FESD

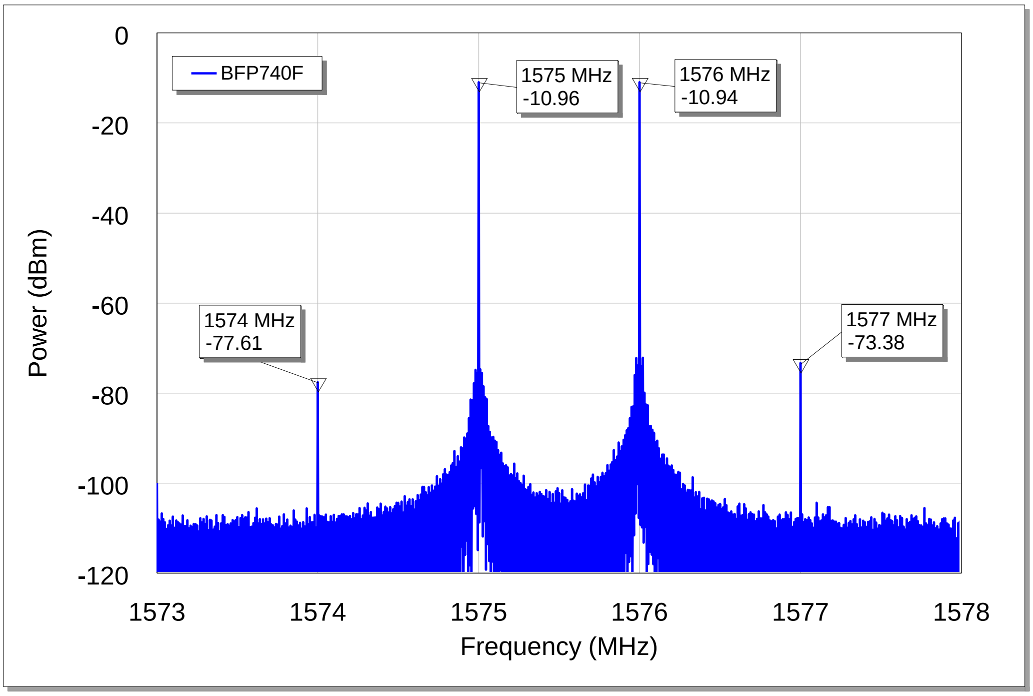

Figure 28 Output third-order intermodulation distortion product of the GNSS LNA with [BFP740F]

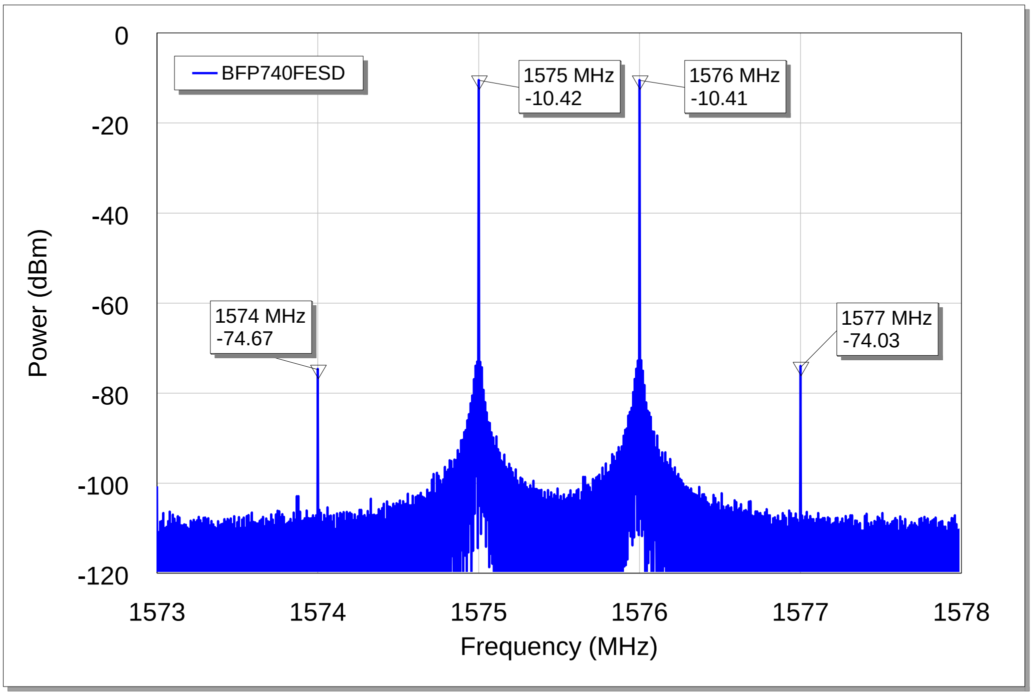

Figure 29 Output third-order intermodulation distortion product of the GNSS LNA with [BFP740FESD]

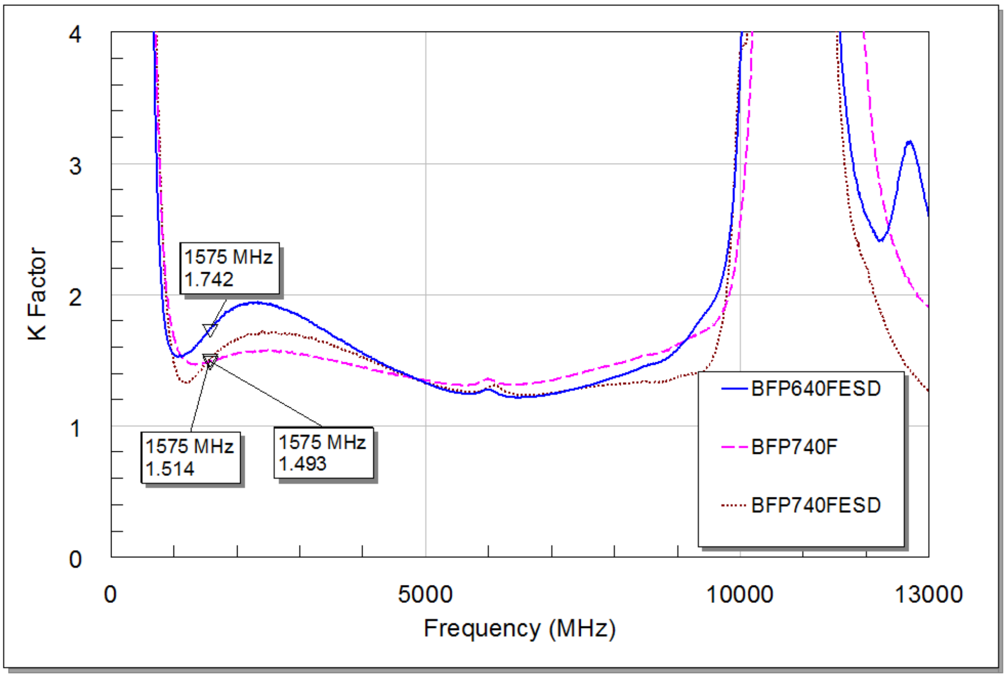

Figure 30 **K-factor measurement of the GNSS LNAs with transistors in small and flat leaded TSFP packages**

4 Wide-band GNSS LNAs with low-noise MMICs

4.1 Performance overview

The following table shows the performance of the wide-band GNSS LNAs with low-noise MMICs measured at 1176 (band L5), 1227 (band L2) and 1575 (band L1) MHz.

Table 5 Summary of measurement results for the wideband GNSS LNAs with low-noise MMICs

Parameter	Symbol	Value						Unit	Notes
Device		BGB707L7ESD			BGB741L7ESD				
Bias voltage	V_{CC}	3.0			3.0			V	
Bias current	I_{CC}	11.9			9.3			mA	
Frequency	f	1176	1227	1575	1176	1227	1575	MHz	
Gain	G	20.5	20.5	19.9	19.7	19.6	19.2	dB	
NF	NF	1.03	1.01	0.99	1.16	1.16	1.14	dB	
Input return loss	RL_{in}	11.7	11.5	10.2	14.2	14.1	13.1	dB	
Output return loss	RL_{out}	9.7	9.7	9.7	22.7	22.5	18.1	dB	
Reverse isolation	ISO_{rev}	27.1	27.0	26.8	23.0	23.0	23.3	dB	
Input 1 dB compression point	IP_{1dB}	-13.9	-14.1	-13.4	-6.5	-6.6	-6.2	dBm	
Output 1 dB compression point	OP_{1dB}	5.6	5.4	5.5	12.2	12.0	12.1	dBm	
Input IP3	IIP_3	-1.3	-2.6	-0.8	5.1	1.9	5.7	dBm	
Output IP3	OIP_3	19.2	17.9	19.1	24.7	21.4	24.9	dBm	P_{IN} = -30 dBm per tone Tone spacing: 1 MHz
Stability	K	>1			>1				Measured from 100 MHz to 13 GHz

4.2 Schematic

The following figure shows the schematic of the wide-band GNSS LNA with low-noise MMIC BGB707L7ESD. In the circuit, the resistor R1 sets up the biasing current. The resistors R2 and R3 stabilize the circuit whose firmness is measured up to 13 GHz. The resistor R4 and the capacitor C5 serve as the negative feedback to improve the input and output impedance matching. The circuit input matching is achieved by the network of capacitors C1, C2 and the inductor L1. The network of L2 and C4 matches the transistor to the output port. The capacitors C2 and C3 serve as the RF bypass.

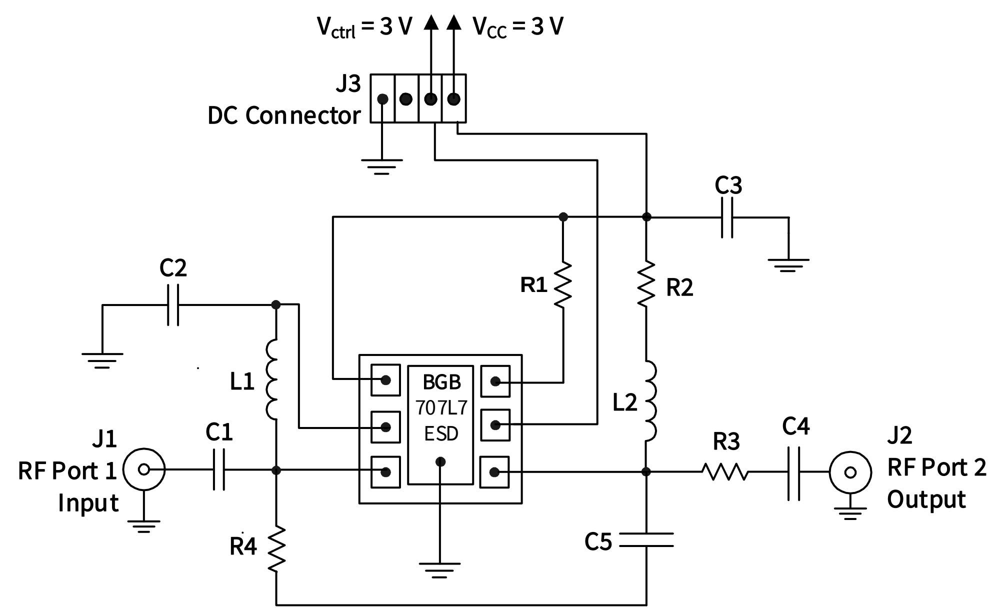

Figure 31 Wide-band GNSS LNA schematic with BGB707L7ESD

The following figure shows the schematic of the wide-band GNSS LNA with low-noise MMIC BGB741L7ESD. In the circuit, the resistor R1 sets up the biasing current. The circuit input matching is achieved by the network of capacitors C1, C2 and the inductor L1. The network of L2 and C4 matches the transistor to the output port. The capacitors C2 and C3 serve as the RF bypass. The stability of the circuit is measured up to 13 GHz.

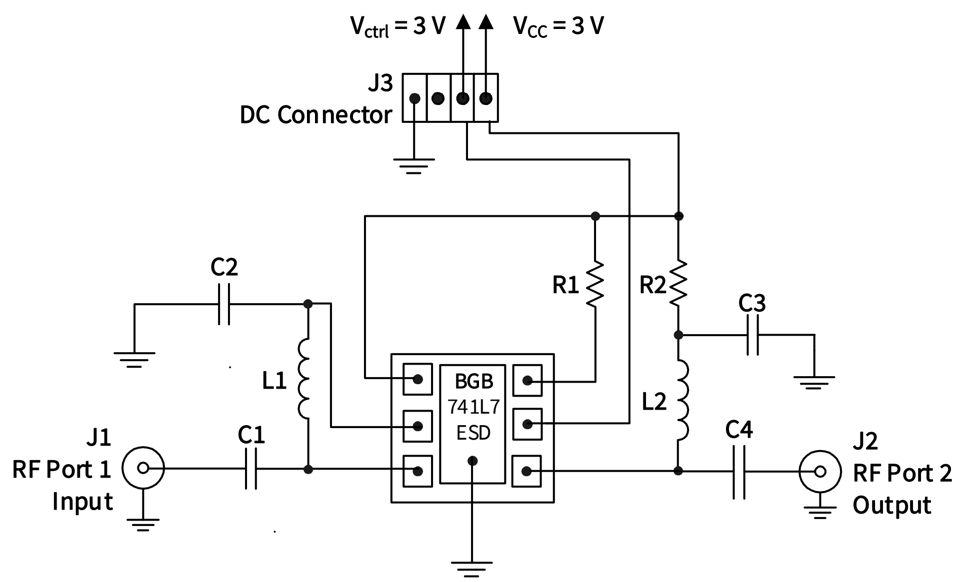

Figure 32 Wide-band GNSS LNA schematic with BGB741L7ESD

4.3 BOM

Table 6 BOM of the wide-band GNSS LNA with BGB707L7ESD

Symbol	Value	Unit	Package	Manufacturer	Comment
Q1	BGB707L7ESD		TSLP-7-1	Infineon	SiGe:C low-noise MMIC
C1	68	pF	0402	Various	Input matching and DC blocking
C2	47	pF	0402	Various	RF decoupling
C3	47	nF	0402	Various	RF decoupling
C4	10	pF	0402	Various	Output matching and DC blocking
C5	10	pF	0402	Various	RF decoupling and DC blocking
R1	820	Ω	0402	Various	Base bias
R2	56	Ω	0402	Various	Stability improvement
R3	15	Ω	0402	Various	Stability improvement
R4	1.2	kΩ	0402	Various	Feedback
L1	22	nH	0402	Murata LQG	Input matching
L2	15	nH	0402	Murata LQG	Output matching

Table 7 BOM of the wide-band GNSS LNA with BGB741L7ESD

Symbol	Value	Unit	Package	Manufacturer	Comment
Q1	BGB741L7ESD		TSLP-7-1	Infineon	SiGe:C low-noise MMIC
C1	47	pF	0402	Various	Input matching and DC blocking
C2	1	µF	0402	Various	RF decoupling
C3	1	µF	0402	Various	RF decoupling
C4	100	pF	0402	Various	Output matching and DC blocking
R1	3.3	kΩ	0402	Various	Base bias
R2	0	Ω	0402	Various	Jumper
L1	33	nH	0402	Murata LQG	Input matching
L2	27	nH	0402	Murata LQG	Output matching

4.4 Evaluation boards and layout information

The wide-band GNSS LNA evaluation board with BGB707L7ESD:

- PCB material: Rogers RO4003C
- PCB marking: BGB7–Family V3.1 M141017

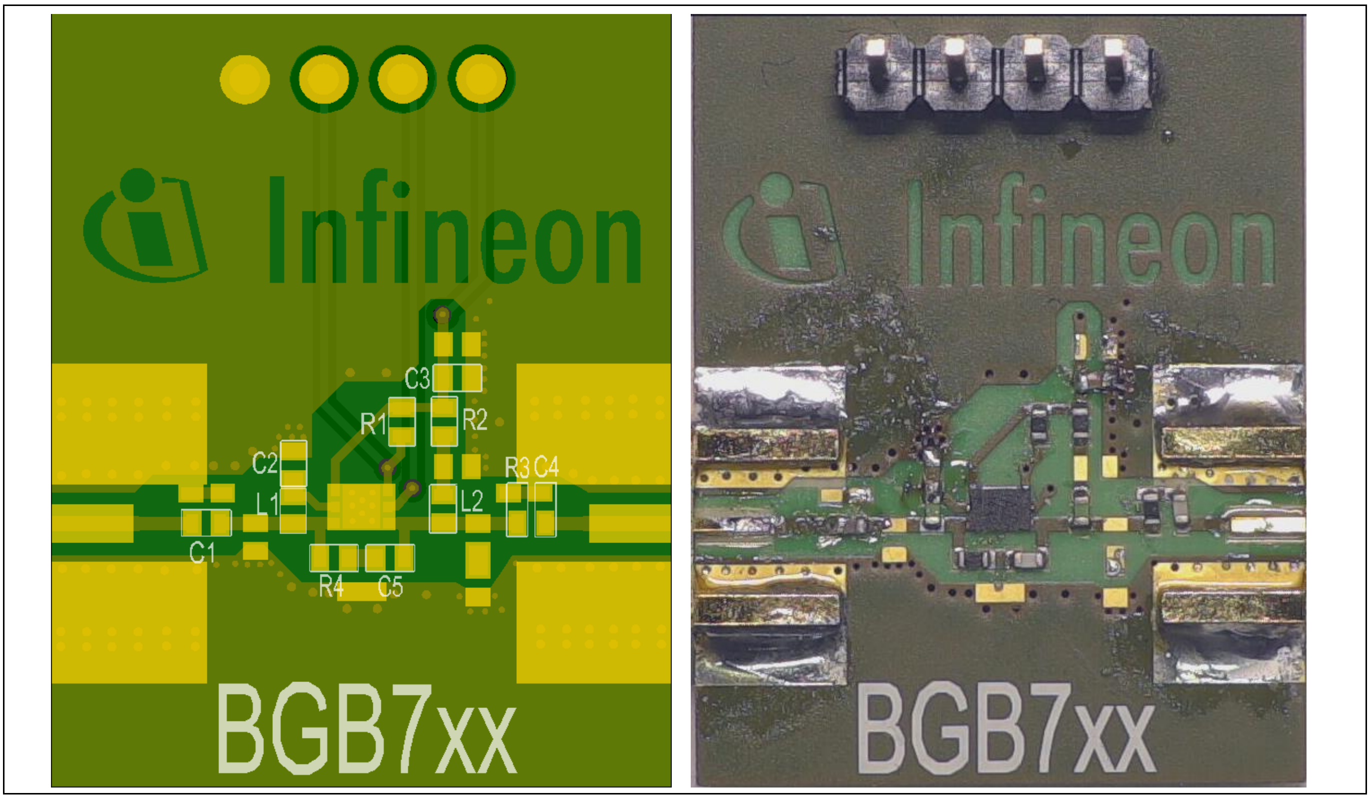

Figure 33 PCB layout and photo of the [BGB707L7ESD](BGB707L7ESD) wide-band GNSS LNA evaluation board

The wide-band GNSS LNA evaluation board with BGB741L7ESD:

- PCB material: Rogers RO4003C
- PCB marking: BGB7–Family V5.2 M170302

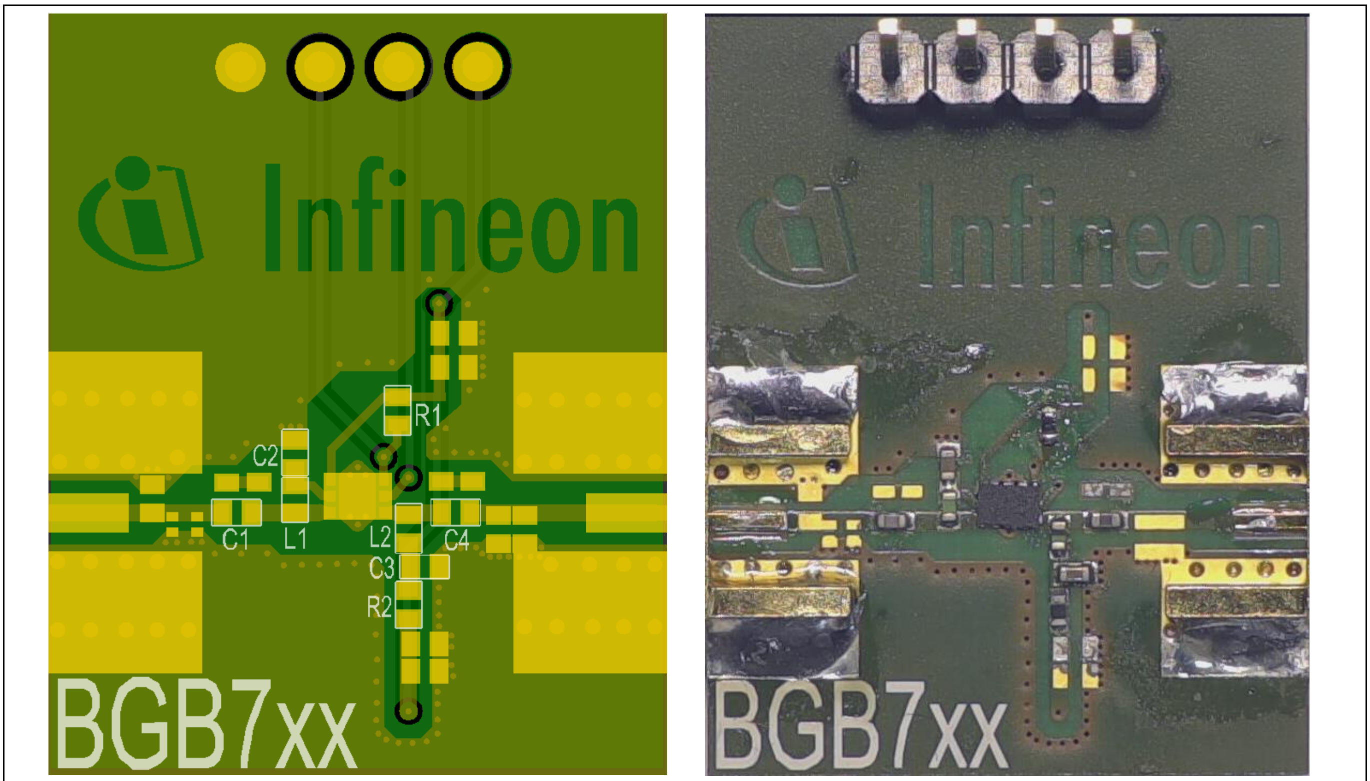

Figure 34 PCB layout and photo of the BGB741L7ESD wide-band GNSS LNA evaluation board

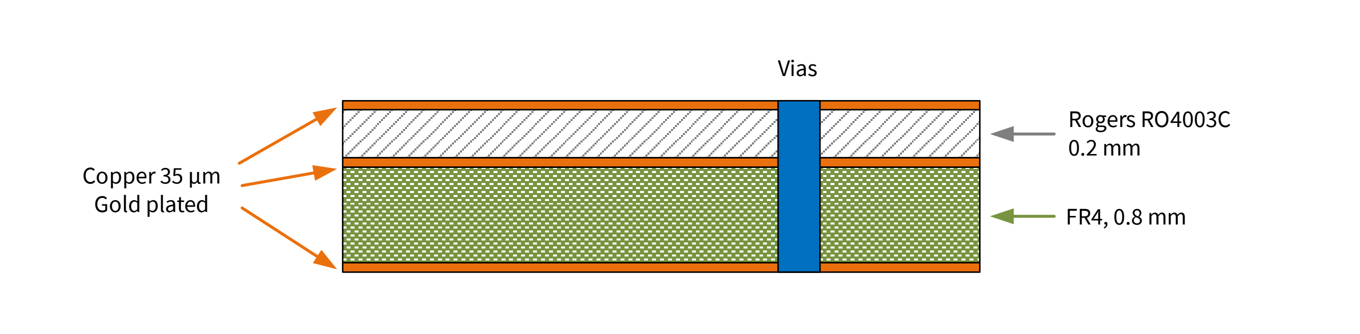

Figure 35 PCB stack information for the evaluation boards M141017 and M170302

4.5 Measurement results of the wide-band GNSS LNAs with low-noise MMICs

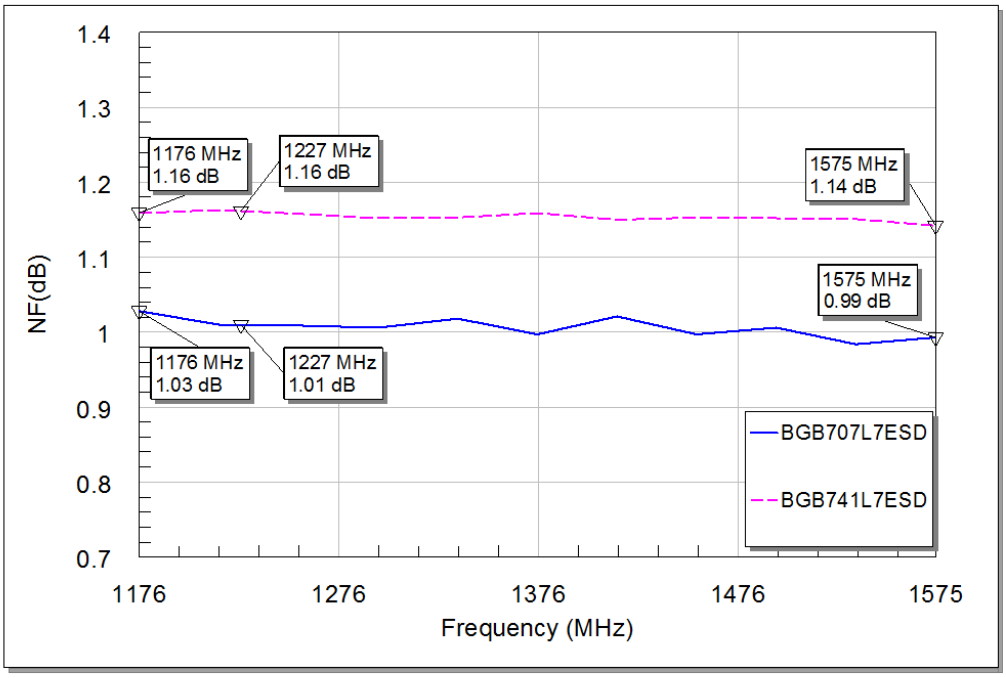

Figure 36 NF measurement of the wide-band GNSS LNAs with low-noise MMICs

Note: The graphs are generated with the AWR EDA software Microwave Office®.

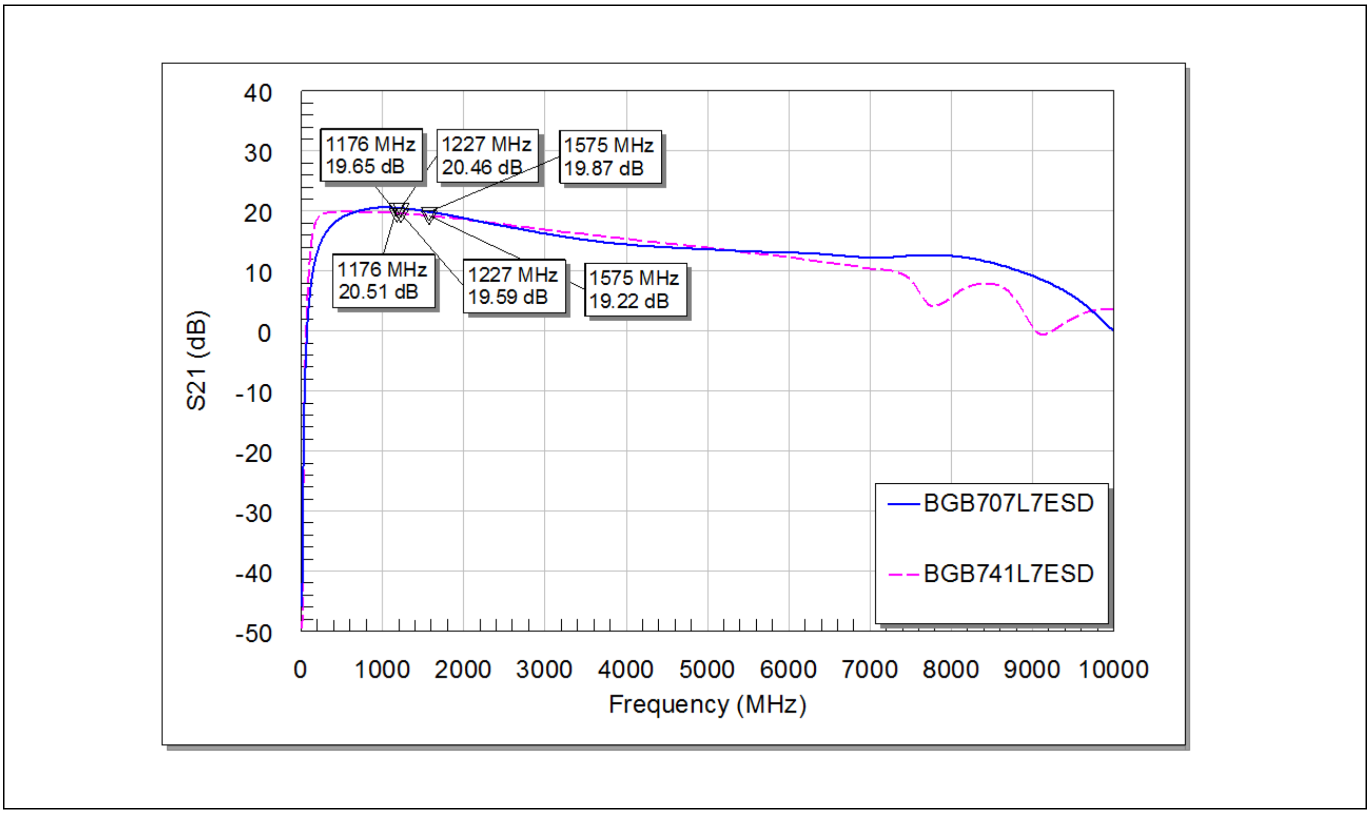

Figure 37 Small signal gain measurement of the wide-band GNSS LNAs with low-noise MMICs

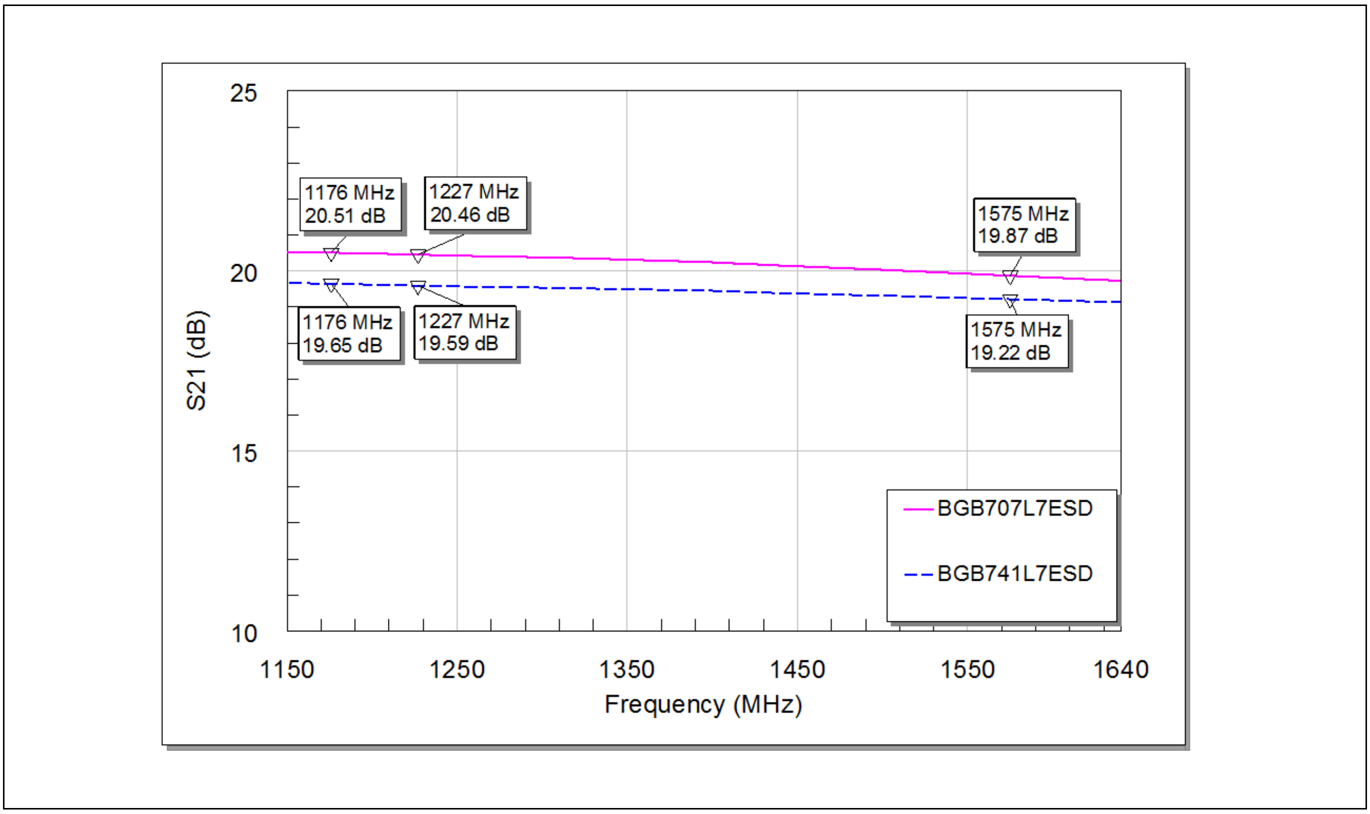

Figure 38 Small signal gain measurement of the wide-band GNSS LNAs with low-noise MMICs (detail view)

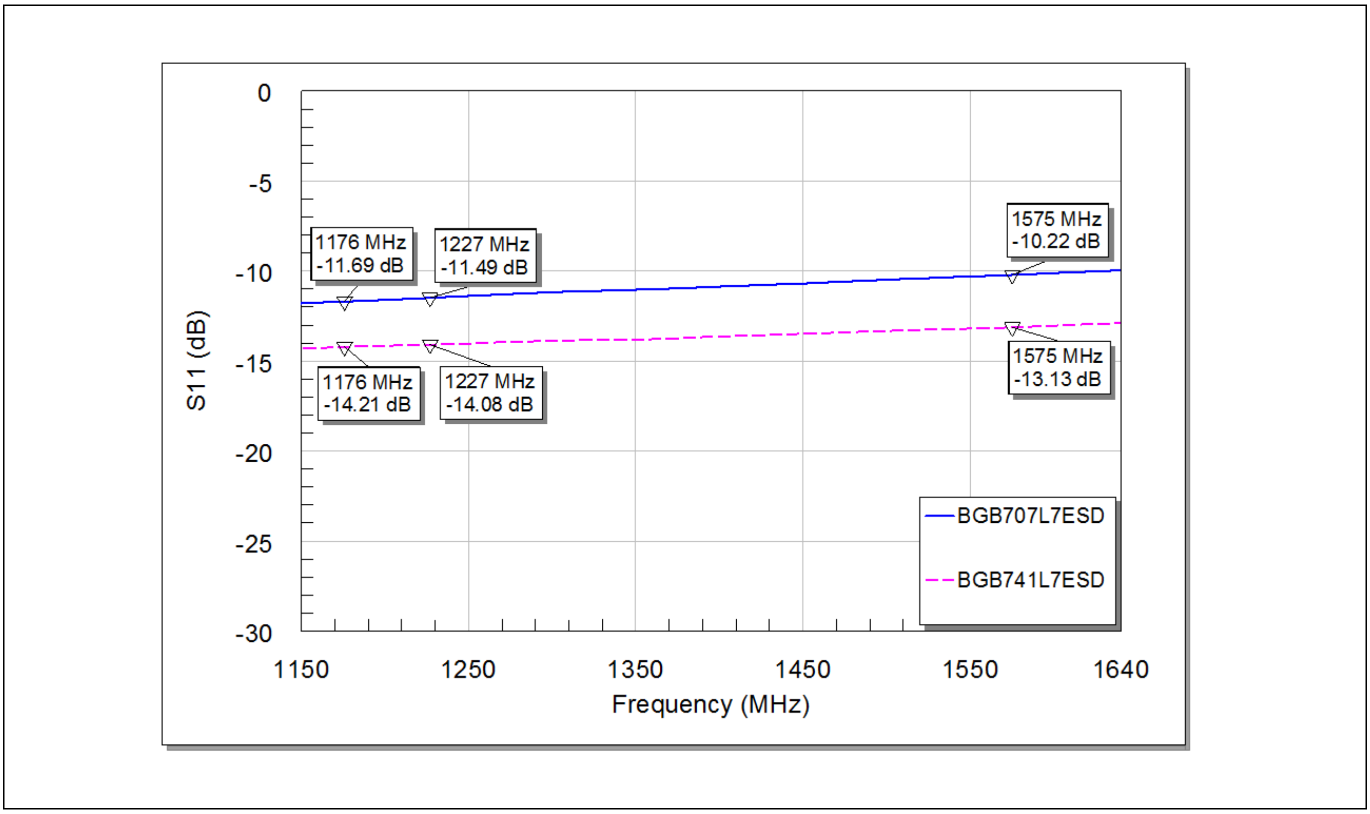

Figure 39 S_{11} measurement of the wide-band GNSS LNAs with low-noise MMICs

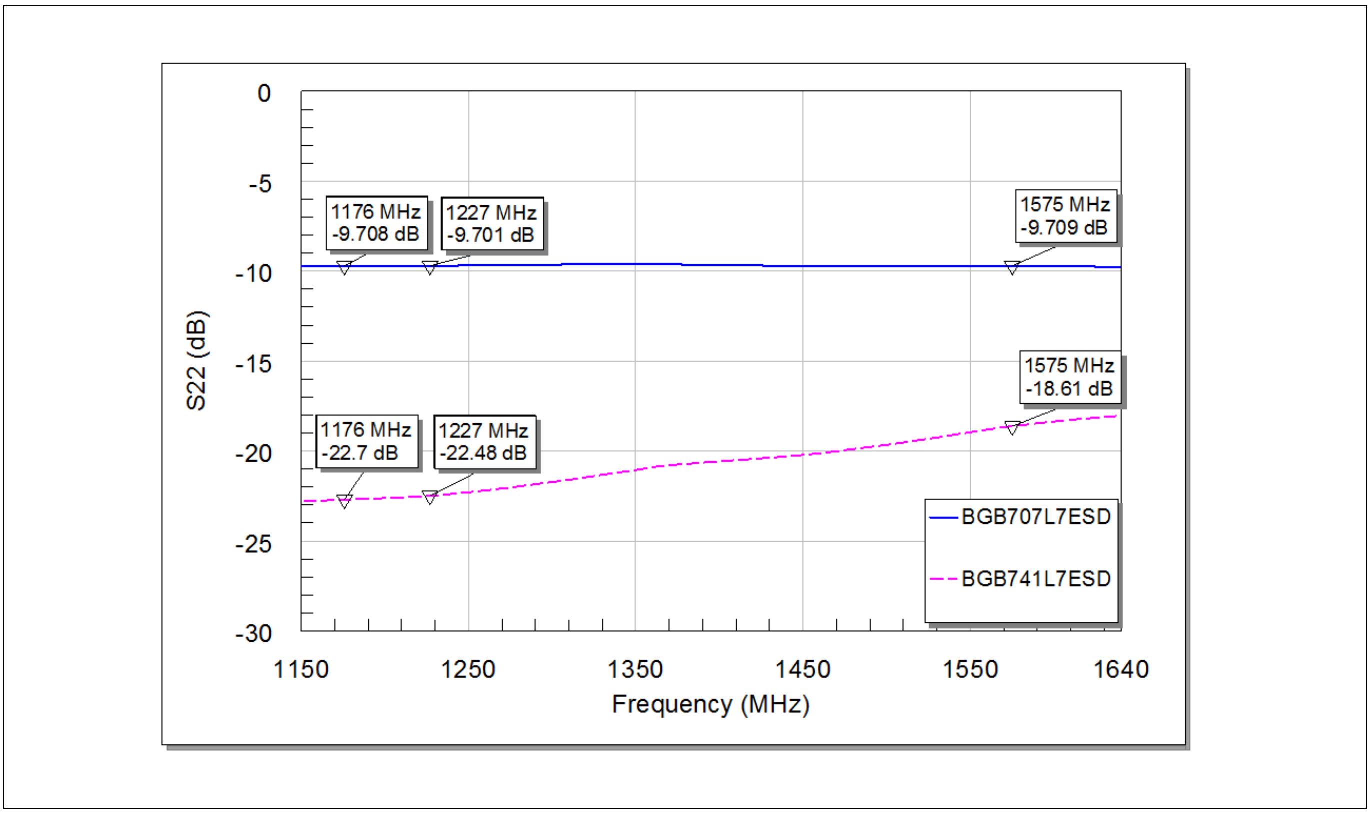

Figure 40 S_{22} measurement of the wide-band GNSS LNAs with low-noise MMICs

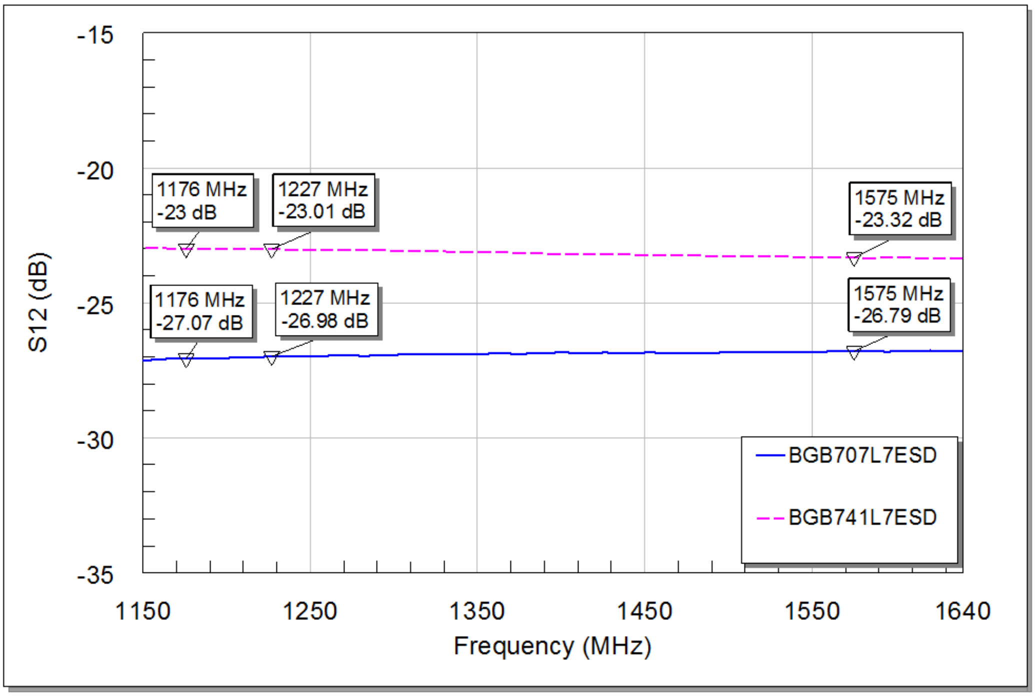

Figure 41 Reverse isolation measurement of the wide-band GNSS LNAs with low-noise MMICs

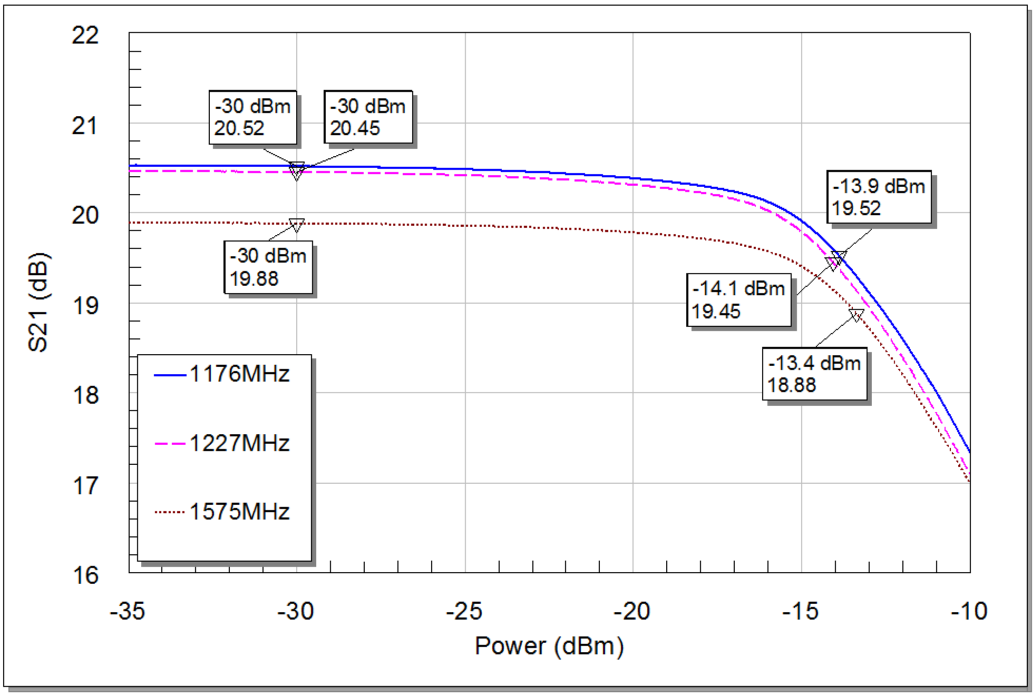

Figure 42 Input 1 dB compression point measurement of the wide-band GNSS LNA with BGB707L7ESD

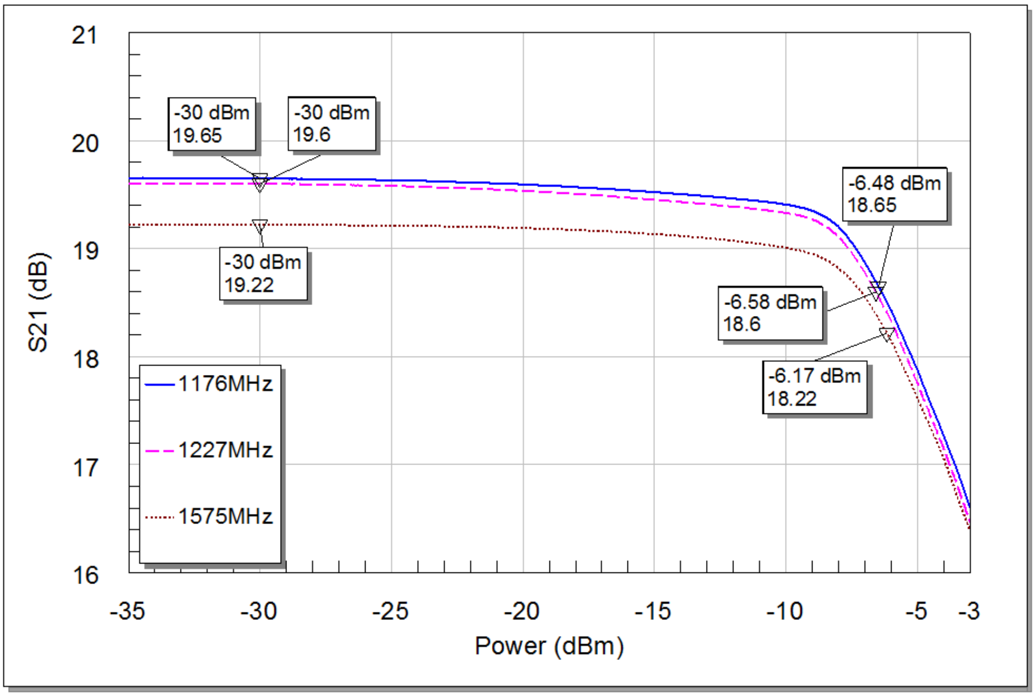

Figure 43 Input 1 dB compression point measurement of the wide-band GNSS LNA with BGB741L7ESD

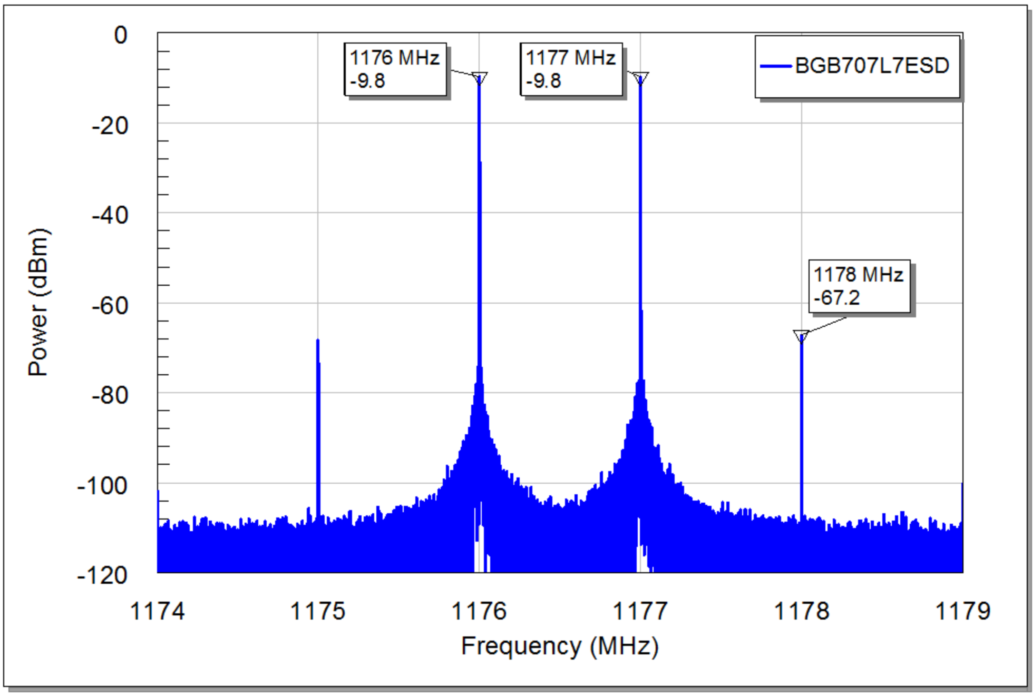

Figure 44 Output third-order intermodulation products at 1176 MHz of the wide-band GNSS LNA with BGB707L7ESD

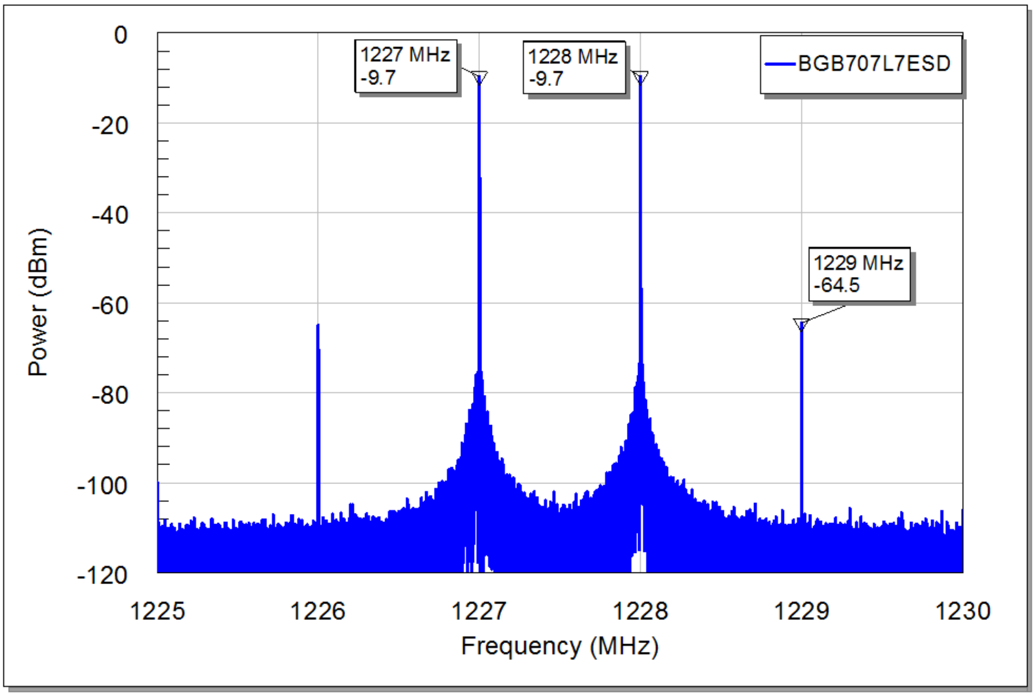

Figure 45 Output third-order intermodulation products at 1227 MHz of the wide-band GNSS LNA with BGB707L7ESD

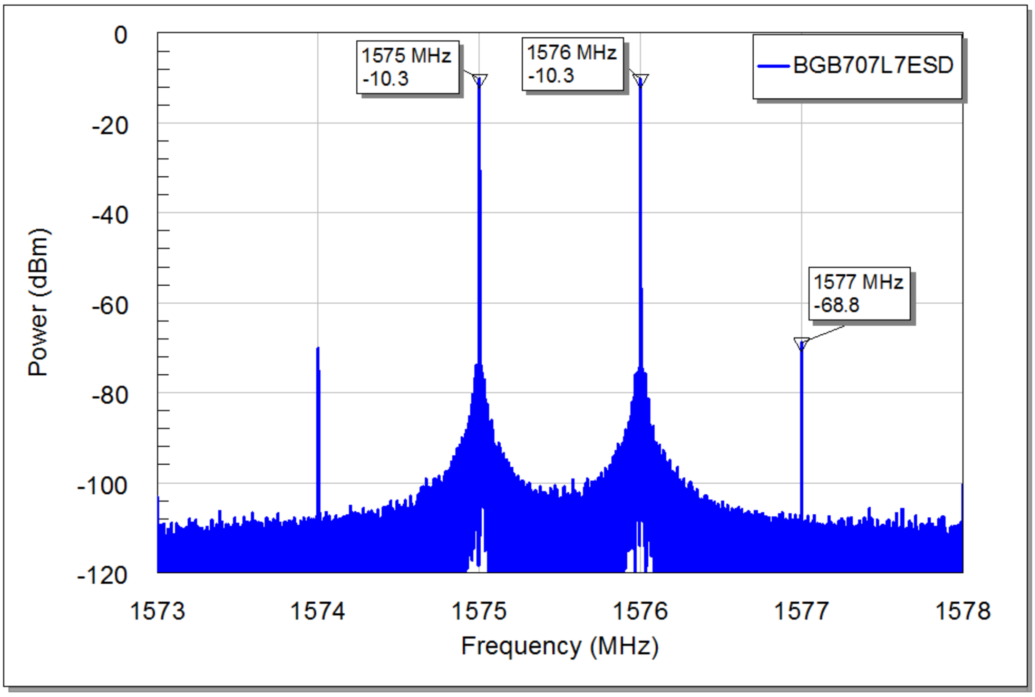

Figure 46 Output third-order intermodulation products at 1575 MHz of the wide-band GNSS LNA with BGB707L7ESD

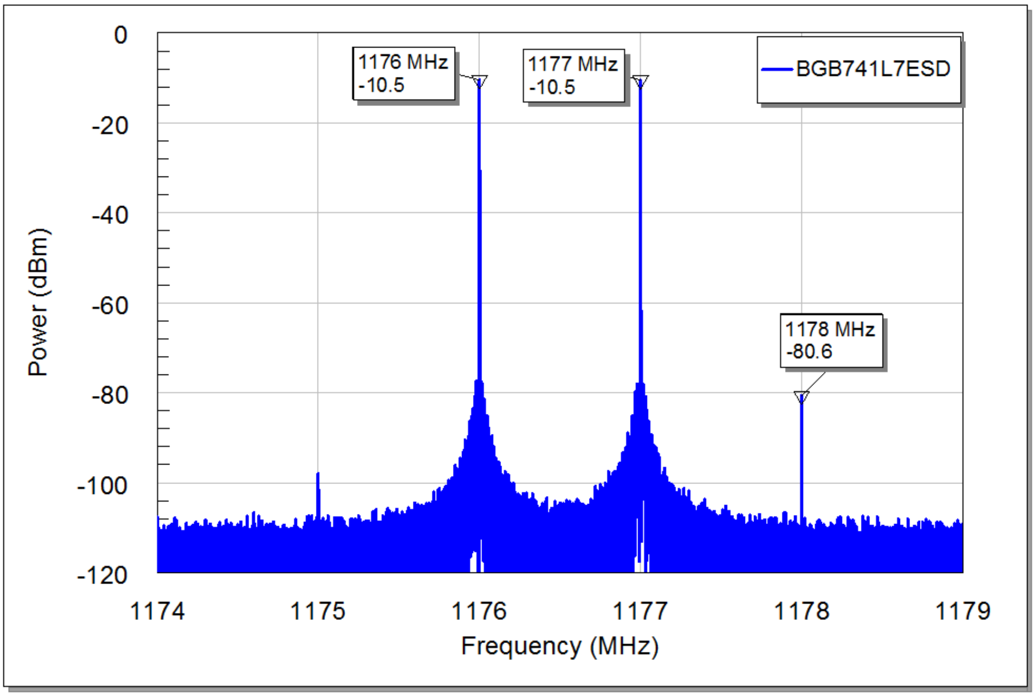

Figure 47 Output third-order intermodulation products at 1176 MHz of the wide-band GNSS LNA with BGB741L7ESD

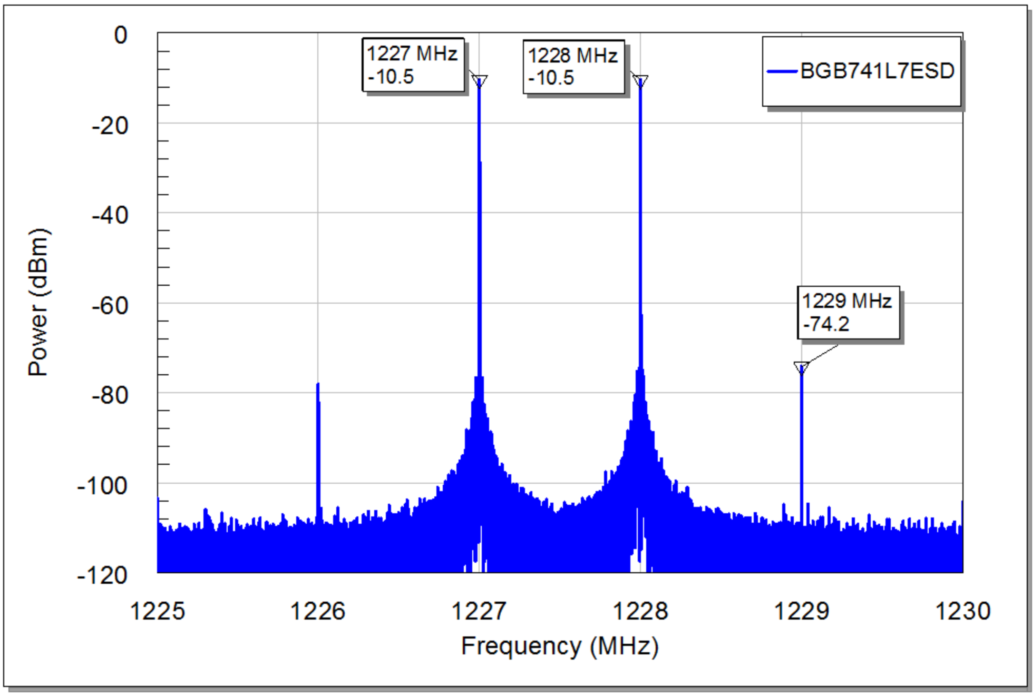

Figure 48 Output third-order intermodulation products at 1227 MHz of the wide-band GNSS LNA with BGB741L7ESD

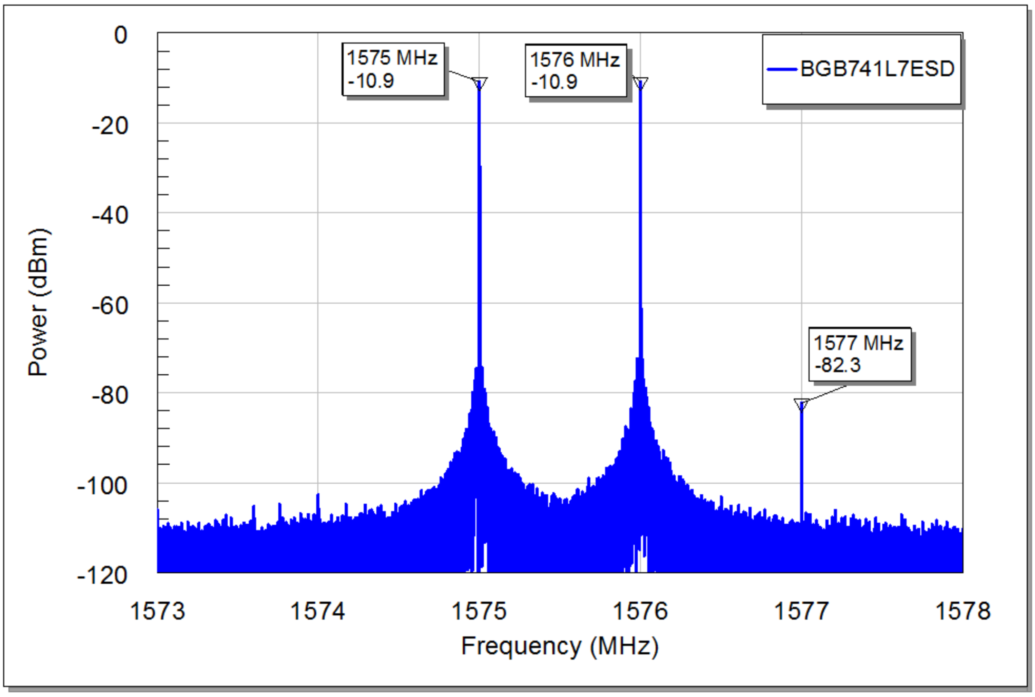

Figure 49 Output third-order intermodulation products at 1575 MHz of the wide-band GNSS LNA with BGB741L7ESD

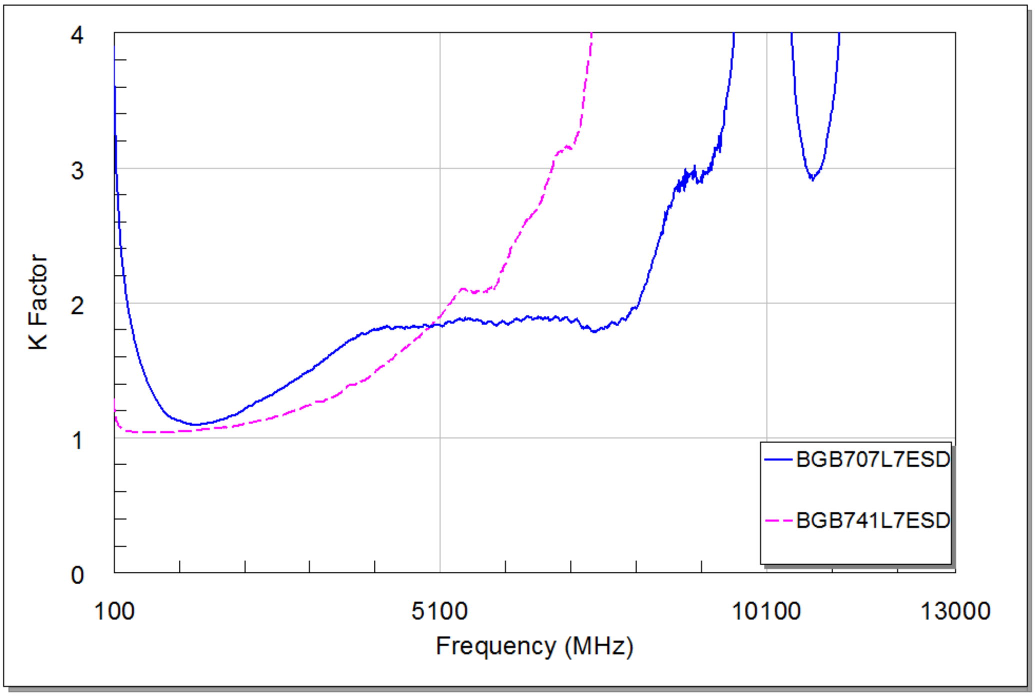

Figure 50 K-factor measurement of the wide-band GNSS LNAs with low-noise MMICs

5 Authors

Mamun Md Abdullah Al, RF application engineer of business unit RF and sensors.

Dr. Jie Fang, RF staff application engineer of business unit RF and sensors.

Revision history

Document version	Date of release	Description of changes

Trademarks

All referenced product or service names and trademarks are the property of their respective owners.

Edition 2018-05-23

Published by

Infineon Technologies AG

81726 Munich, Germany

Do you have a question about this document?

Email: erratum@infineon.com

Document reference
AN_1805_PL32_1806_113119